



# Near-Integrability and Recurrence in FPU-Cells

Ferdinand Verhulst

*Mathematisch Instituut, P. O. Box 80.010,  
 3508TA Utrecht, Netherlands*

Received March 3, 2016; Revised September 21, 2016

In a neighborhood of stable equilibrium, we consider the dynamics for at least three degrees-of-freedom (dof) Hamiltonian systems (2 dof systems are not ergodic in this case). A complication is that the recurrence properties depend strongly on the resonances of the corresponding linearized system and on quasi-trapping. In contrast to the classical FPU-chain, the *inhomogeneous* FPU-chain shows nearly all the principal resonances. Using this fact, we construct a periodic FPU-chain of low dimension, called a FPU-cell. Such a cell can be used as a building block for a chain of FPU-cells, called a cell-chain. Recurrence phenomena depend strongly on the physical assumptions producing specific Hamiltonians; we demonstrate this for the  $1 : 2 : 5$  resonance, both general and for the FPU case; this resonance shows dynamics on different timescales. In addition we will study the relations and recurrence differences between several FPU-cells and a few cell-chains in the case of the classical near-integrable FPU-cell and of chaotic cells in  $3 : 2 : 1$  resonance.

*Keywords:* Hamiltonian; FPU-chain; quasi-trapping; resonance.

## 1. Introduction

The purpose of this paper is to study recurrence in Hamiltonian systems with three or more dof near stable equilibrium. We will show that near-integrability, i.e. integrability of a certain normal form, will produce more regular recurrence phenomena than chaotic behavior of the corresponding normal form. Our paper is focused on connected, low-dimensional FPU-cells and, only for comparison, on a few more general Hamiltonians. The analysis can be turned around to use recurrence phenomena as a “smoking gun” for phase-space diffusion and prominent chaotic behavior.

The Fermi–Pasta–Ulam (FPU) chain or lattice is an  $n$  dof Hamiltonian system that models a chain of oscillators with nearest-neighbor interaction, see [Fermi *et al.*, 1955; Ford, 1992], and for recent references [Christodoulidi *et al.*, 2010]. In the classical case, also called the symmetric case in [Brugge-man & Verhulst, 2015], all the masses  $m_i$ ,  $i = 1, \dots, n$  of the chain are equal. In a seminal paper

[Chechin & Sakhnenko, 1998] group-theoretical methods were used for systems with certain symmetries. From irreducible representations of the symmetry group the authors concluded the existence of specific dynamical regimes (called *bushes*) of essentially lower dimension than the dimension of the original systems. The theory was developed in [Chechin & Sakhnenko, 1998] both for Hamiltonian and non-Hamiltonian systems with a number of physical applications.

Independently, in [Poggi & Ruffo, 1997] the periodic FPU  $\beta$ -chain was considered for which special periodic solutions and two-mode invariant manifolds were found. The paper by Chechin and Sakhnenko [1998] was continued in [Chechin *et al.*, 2002] to find invariant manifolds (bushes) in classical periodic, monatomic FPU-chains. The analysis leads to the existence of a wide range of multi-mode invariant manifolds that includes the results in [Poggi & Ruffo, 1997]. Exploiting symmetries, a number of new invariant manifolds for the classical,

periodic FPU-chain were given in [Rink, 2001]; the presence of invariant manifolds imposes restrictions on the phase-flow and so influences the recurrence properties.

Inhomogeneous nonlinear FPU-chains were studied in [Bruggeman & Verhulst, 2015] with emphasis, as a start, on the case of four particles in a so-called  $\alpha$ -chain with mass distribution producing the 3 : 2 : 1 resonance. We will call such a FPU-chain of low dimension a FPU-cell and, following Verhulst [2015b], we will connect these cells producing a cell-chain; for an example see Fig. 1,

but we will restrict ourselves in the explicit examples to at most two cells. More complicated chains are to be considered in future explorations.

The Hamiltonian depends on momenta  $p$  and positions  $q$ ; it is of the form:

$$H(p, q) = H_2(p, q) + \varepsilon H_3(q),$$

with quadratic  $H_2$ , cubic  $H_3$  and where the usual  $\alpha$  is replaced by the small parameter  $\varepsilon$ . The expression for the quadratic part of the Hamiltonian  $H_2$  is in the case of a FPU-cell with 4 degrees-of-freedom (dof):

$$H_2 = \frac{1}{2} \sum_{i=1}^4 a_i p_i^2 + \frac{1}{2} [(q_2 - q_1)^2 + (q_3 - q_2)^2 + (q_4 - q_3)^2 + (q_1 - q_4)^2]. \quad (1)$$

The cubic terms are in this case:

$$H_3 = \frac{1}{3} [(q_2 - q_1)^3 + (q_3 - q_2)^3 + (q_4 - q_3)^3 + (q_1 - q_4)^3]. \quad (2)$$

Then, for one periodic inhomogeneous FPU  $\alpha$ -chain with masses  $m_i$ ,  $i = 1, \dots, 4$  and 4 dof we have, putting  $a_i = 1/m_i$ , the FPU-cell described by the equations of motion:

$$\begin{cases} \dot{q}_1 = v_1, & \dot{v}_1 = [-2q_1 + q_2 + q_4 - \varepsilon((q_1 - q_4)^2 - (q_2 - q_1)^2)]a_1, \\ \dot{q}_2 = v_2, & \dot{v}_2 = [-2q_2 + q_3 + q_1 - \varepsilon((q_2 - q_1)^2 - (q_3 - q_2)^2)]a_2, \\ \dot{q}_3 = v_3, & \dot{v}_3 = [-2q_3 + q_4 + q_2 - \varepsilon((q_3 - q_2)^2 - (q_4 - q_3)^2)]a_3, \\ \dot{q}_4 = v_4, & \dot{v}_4 = [-2q_4 + q_1 + q_3 - \varepsilon((q_4 - q_3)^2 - (q_1 - q_4)^2)]a_4. \end{cases} \quad (3)$$

We find it convenient to use the velocity  $v_i$  with  $p_i = m_i v_i$ ,  $\varepsilon$  is a positive, small parameter.

Apart from the Hamiltonian  $H$  we have as a second (translational) momentum integral of system (3):

$$m_1 v_1 + m_2 v_2 + m_3 v_3 + m_4 v_4 = \text{const} \quad (4)$$

$H_2$  is a first integral of system (3) linearized near the origin, but it is also a first integral of the normal form of the full system (3). This means that when using  $H_2$  from the solutions of the truncated normal form indicated by:

$$\bar{H}(p, q) = H_2(p, q) + \varepsilon \bar{H}_3(p, q),$$

we obtain an  $O(\varepsilon)$  approximation of the (exact)  $H_2(p(t), q(t))$  valid for all time; for a proof see [Sanders *et al.*, 2007, Chapter 10]. Using the expression  $H_2(p(t), q(t))$  for the solutions of the full system (3) demonstrates the accuracy of the normal form solutions and gives an impression of the nature of the dynamics. For an illustration by geometric numerical integration see [Hairer *et al.*, 2006, p. 479].

Choosing the initial conditions assigns a value to an integral. For the Hamiltonian this constant value will be indicated by  $E$  (energy), for  $H_2$  we use  $E_0$ , for other integrals we use  $E_1, E_2, \dots$ .

It was shown in [Rink & Verhulst, 2000], that in the classical periodic FPU problem with four identical particles the normal form of the system is integrable, see also [Rink, 2001]. The implication is that for  $\varepsilon$  small, the Lebesgue measure of chaos is  $O(\varepsilon)$  in this classical case.

In the sequel we will discuss a FPU chain with four particles as a FPU-cell, and we will construct several FPU cell-chains. Depending on the choice of interactions and the number of cells, many cell-chains are possible. We show an example consisting of three cells depicted in Fig. 1.

Most Hamiltonian systems are *nonintegrable* but to characterize their dynamics this concept is too general. For instance near stable equilibrium, two dof systems will be nonintegrable but the chaotic orbits are restricted to exponentially small sets with respect to the energy; on the other hand,

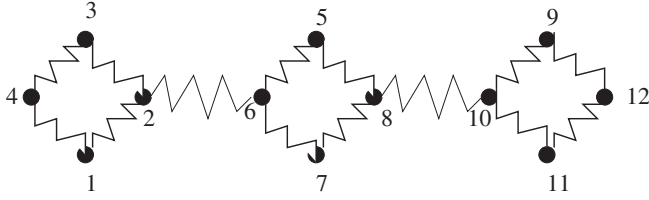


Fig. 1. A cell-chain of three FPU-cells, each consisting of four particles.

the 3 : 2 : 1 resonance to be discussed later shows large-scale chaos near stable equilibrium. Tools to describe nonintegrable systems are the asymptotic behavior of normal form integrals like  $H_2$  as used in [Verhulst, 2015a] and the recurrence theorem. In Sec. 3, we will discuss this theorem. In Sec. 4, we will consider recurrence for the 1 : 2 : 5 resonance as a perturbed integrable system both for the general case and for a FPU-cell. This resonance is of special interest as it shows dynamics on more than one long timescale. In Sec. 5, we will discuss classical FPU-cells (equal masses) to demonstrate the relation between near-integrability and recurrence. Section 6 discusses the case of a chaotic FPU-cell that arises for the 3 : 2 : 1 resonance.

A remark about numerics and precision. We have used ode78 of MATCONT under MATLAB for our numerical integrations. The integrations were repeated with increasing accuracy until a stable picture appeared; for most integrations relative precision  $e^{-17}$ , and absolute precision  $e^{-20}$  were needed. Another check is the calculation of the normal form integral  $H_2$  mentioned above and discussed in Sec. 3. This quantity is conserved to  $O(\varepsilon)$  for all time and can serve as an additional check on the accuracy of integration, see [Sanders *et al.*, 2007; Hairer *et al.*, 2006].

## 2. The Equations of Motion for a Cell-Chain

Consider a FPU-cell with 4 dof and as an example the arrangement of Fig. 1. The three cells interact by the mass points 2, 6, 8, 10 with displacements  $q_2, q_6, q_8, q_{10}$  and a choice of masses  $m_i, i = 1, \dots, 4$ . When considering a special resonance in a cell, like the 3 : 2 : 1 resonance, the interaction of the cells should result only in a slight detuning. The quadratic part of the Hamiltonian (1) transformed to  $(q, v)$  coordinates for two cells extends to:

$$\left\{ \begin{aligned} H_2 &= \frac{1}{2} \sum_{i=1}^{12} \frac{v_i^2}{a_i} + \frac{1}{2} [(q_2 - q_1)^2 + (q_3 - q_2)^2 + (q_4 - q_3)^2 + (q_1 - q_4)^2] \\ &\quad + \frac{1}{2} \varepsilon c_1 (q_2 - q_6)^2 + \frac{1}{2} [(q_6 - q_5)^2 + (q_7 - q_6)^2 + (q_8 - q_7)^2 + (q_5 - q_8)^2] \end{aligned} \right. \quad (5)$$

with  $a_i = a_{i+4}, i = 1, \dots, 4$ ;  $\varepsilon$  scales the nonlinearities,  $\varepsilon c_1$  determines the magnitude of interaction. The cubic part for one cell is:

$$H_3 = \frac{\varepsilon}{3} \sum_{i=1}^4 (q_{i+1} - q_i)^3. \quad (6)$$

The equations of motion become for two cells:

$$\left\{ \begin{aligned} \dot{q}_1 &= v_1, & \dot{v}_1 &= [-2q_1 + q_2 + q_4 - \varepsilon((q_1 - q_4)^2 - (q_2 - q_1)^2)]a_1, \\ \dot{q}_2 &= v_2, & \dot{v}_2 &= [-2q_2 + q_3 + q_1 - \varepsilon c_1(q_2 - q_6) - \varepsilon((q_2 - q_1)^2 - (q_3 - q_2)^2)]a_2, \\ \dot{q}_3 &= v_3, & \dot{v}_3 &= [-2q_3 + q_4 + q_2 - \varepsilon((q_3 - q_2)^2 - (q_4 - q_3)^2)]a_3, \\ \dot{q}_4 &= v_4, & \dot{v}_4 &= [-2q_4 + q_1 + q_3 - \varepsilon((q_4 - q_3)^2 - (q_1 - q_4)^2)]a_4, \\ \dot{q}_5 &= v_5, & \dot{v}_5 &= [-2q_5 + q_6 + q_8 - \varepsilon((q_5 - q_8)^2 - (q_6 - q_5)^2)]a_1, \\ \dot{q}_6 &= v_6, & \dot{v}_6 &= [-2q_6 + q_7 + q_5 + \varepsilon c_1(q_2 - q_6) - \varepsilon((q_6 - q_5)^2 - (q_7 - q_6)^2)]a_2, \\ \dot{q}_7 &= v_7, & \dot{v}_7 &= [-2q_7 + q_8 + q_6 - \varepsilon((q_7 - q_6)^2 - (q_8 - q_7)^2)]a_3, \\ \dot{q}_8 &= v_8, & \dot{v}_8 &= [-2q_8 + q_5 + q_7 - \varepsilon c_2(q_8 - q_{10}) - \varepsilon((q_8 - q_7)^2 - (q_5 - q_8)^2)]a_4. \end{aligned} \right. \quad (7)$$

The momentum integral for this system is:

$$\sum_{i=1}^8 m_i v_i = \text{const} \quad (8)$$

This integral can be used to reduce system (7) by one dof.

### 3. The Recurrence Theorem

The recurrence theorem for volume-preserving maps was formulated by Poincaré in 1890 in his prize essay for king Oscar II of Sweden and Norway; it can also be found in [Poincaré, 1892, 1893, 1899, Vol. 3]. Modern formulations are in terms of measure-preserving maps.

#### 3.1. Hamiltonian systems

The phase-flow induced by a time-independent Hamiltonian is volume-preserving. The recurrence theorem implies, loosely formulated, that for Hamiltonian systems on a bounded energy manifold, nearly all solutions return after a finite time  $T_r$  arbitrarily close to their original position in phase-space. Analysis of recurrence adds to our understanding of the dynamics; we will restrict ourselves to time-independent Hamiltonian systems. A more precise formulation in this case is:

**Proposition 3.1.** The Poincaré Recurrence Theorem. *Consider the phase-flow  $F$  of a dynamical system induced by the Hamiltonian function  $H(p, q)$ ,  $(p, q) \in \mathbb{R}^{2n}$ . A bounded energy manifold  $M$  determined by  $H(p, q) = E$  (real constant) has a subset  $D_0 \subset M$  with positive measure. Nearly all points  $P$  in  $D_0$  (in the sense of measure theory) will return under the map  $F$  after a finite time arbitrarily close to  $P$  in  $D_0$ .*

*Remark.* A set  $W \subset M$  consisting of points that do not return to  $W$  under the map  $F$  has measure zero. Examples are homoclinic and heteroclinic solutions. Other solutions with this property will be called wandering.

For a 1 dof system on a bounded domain, recurrence is trivial as under these conditions nearly all solutions are periodic. For 2 dof systems that are integrable, recurrence behavior is relatively simple near a stable periodic solution. In nearly-integrable 2 dof systems a similar result can be obtained using the KAM theorem, but in general this is already not so easy for chaotic 2 dof systems.

#### 3.2. A crude upper bound for recurrence

To measure recurrence for a system of FPU-cells we will start with positive energy only in the first cell and consider recurrence within this cell and energy exchange between the FPU-cells. We will use the Euclidean norm; for a system of two cells, this becomes:

$$\left\{ \begin{aligned} d &= \left( \sum_{i=1}^4 (q_i(t) - q_i(0))^2 + (v_i(t) - v_i(0))^2 \right) \\ &+ e_1 \sum_{i=5}^8 ((q_i(t) - q_i(0))^2 + (v_i(t) - v_i(0))^2). \end{aligned} \right. \quad (9)$$

In the sequel we will take  $v_i(0) = 0$ ,  $i = 1, \dots, 8$ ; one can choose to have initial velocity conditions nonzero, but it makes sense to keep the momentum integral (8) zero. In the case of one cell,  $e_1 = 0$ , for two cells  $e_1 = 1$ . It would be natural to apply weights, based on the masses, to the displacements in the distance  $d$  but this does not change the picture qualitatively. Another aspect is that the Euclidean distance  $d$  does *not* present a fixed time of recurrence. For a fixed value of  $d$ , we will find a number of times for which the domain with size  $d$  is traversed. If the initial conditions are very close to stable equilibrium or, with respect to Hamiltonian (10), if the nonlinear terms scaled by  $\varepsilon$  are very small, this number of times of passage through the domain with size  $d$  will be larger. We shall see in our examples, for instance in Fig. 2, that for small nonlinearities the orbital behavior that corresponds with approach to the  $d = 0$  axis is located in  $V$ -shaped domains, they become larger as  $\varepsilon$  decreases. This is natural as for  $\varepsilon = 0$  the system is linear and recurrent on an  $O(1)$  timescale. As we shall see, in systems with integrable normal form, the drift along the torus is characterized by a timescale of order  $1/\varepsilon^r$  ( $r$  a real positive number). So for very small values of  $\varepsilon$  we should adjust our criterion allowing for the size of the  $V$ -shaped regions; in the sequel we will not pursue this idea. For values of  $\varepsilon$  that are not extremely small, the  $V$ -shaped regions will be thin tongues that easily produce a recurrence estimate (see for instance Figs. 4 and 5).

We conclude that the recurrence time  $T_r$  for a given Hamiltonian system is not a fixed number, it depends on its specific phase-flow, the initial

conditions and the recurrence accuracy  $d$  (corresponding with a sphere around the initial position). It is possible to give an upper bound for the values of  $T_r$  but, as we shall see, this is not always helpful. We stress that these qualifications about recurrence were known to Poincaré and that the upper bound to be derived below should not be called “Poincaré recurrence time”.

Consider a time-independent Hamiltonian expanded in the form

$$H(p, q) = H_2(p, q) + \varepsilon H_3(p, q) + \varepsilon^2 H_4(p, q) + \cdots, \quad (10)$$

where the index  $i$  indicates the degree of the homogeneous polynomials  $H_i(p, q)$ ,  $i = 2, 3, \dots$ . Assume that  $H_2(p, q)$  is Morse at  $(p, q) = (0, 0)$  and that the origin is a stable equilibrium of the equations of motion.

The parameter  $\varepsilon$  usually arises by scaling  $p \rightarrow \varepsilon p$ ,  $q \rightarrow \varepsilon q$  and dividing by  $\varepsilon^2$ . For many applications of  $n$  dof time-independent Hamiltonians near stable equilibrium with phase-flow on a compact energy manifold such as (10) with energy  $E = E_0 + O(\varepsilon)$ , this manifold is topologically  $S^{2n-1}$ , a sphere in  $\mathbb{R}^{2n}$  with radius  $R = \sqrt{E_0} + O(\varepsilon)$ . The compactness holds in general below a certain critical value of the energy. If the eigenvalues of equilibrium are all of the same magnitude, the actual energy manifold is approximated by this hypersphere. Such a sphere has an area proportional to  $R^{2n-1}$ . To approximate the energy manifold by a hypersphere makes sense only if we are not too far from stable equilibrium and if the spectrum near equilibrium has not extremely large or small elements. A hypersphere with dimension  $(2n - 1)$  embedded in the energy manifold around the initial conditions with radius  $d \ll R$ , has a volume proportional to  $d^{2n-1}$ . We summarize the results near stable equilibrium:

**Proposition 3.2.** *If an orbit of the system induced by Hamiltonian (10) reaches a size  $d$  neighborhood of each point on a bounded energy manifold near stable equilibrium (the worst case), we have for the upper bound  $L$  of the recurrence time  $T_d$ :*

$$\begin{aligned} L &= O\left(\frac{R^{2n-1}}{d^{2n-1}}\right) \quad \text{or} \\ L &= O\left(\frac{E_0^{n-1/2}}{d^{2n-1}}\right) \quad \text{as } d \rightarrow 0. \end{aligned} \quad (11)$$

We assume that the approximate energy  $E_0$  is an  $O(1)$  quantity. The estimate (11) does not take into account that possibly additional integrals of the Hamiltonian exist or that we are in a near-integrable case; in such a case the estimate for  $L$  is too pessimistic. For instance, in the case of a chain of FPU-cells as in Fig. 1 we have the additional integral (8) which enables us to reduce the system with one dof.

So for one FPU-cell of 4 dof we reduce to 3 dof and  $L = O(1/d^5)$ , for two cells to 7 dof and  $L = O(1/d^{13})$ , for three cells to 11 dof and  $L = O(1/d^{21})$ . These estimates are valid without any additional knowledge about the dynamics of the FPU-cells; we will see that in the near-integrable cases like the classical one, the estimates are far too crude.

### 3.3. Dynamics affecting recurrence

The recurrence depends on the number of dof, the initial conditions and the particular dynamics of the system under consideration. We will compare cell-chains built from classical, near-integrable FPU-cells and chains built from chaotic FPU-cells. In the near-integrable cases (e.g. the classical FPU-cell) the recurrence times are smaller as the invariant manifolds restrict the drifting off of the solutions. However, increasing the number of dof weakens this argument because of quasi-trapping. We discuss the two mechanisms:

#### (1) Separation by invariant manifolds

There is a large qualitative and quantitative difference between two and more dof, *so calculations for two dof are only to some extent typical*. Consider as an example:

$$\begin{cases} \ddot{q}_1 + 4q_1 = \varepsilon q_2^2, \\ \ddot{q}_2 + q_2 = 2\varepsilon q_1 q_2. \end{cases} \quad (12)$$

It is well-known that for  $\varepsilon$  small, the normal form of system (12) is integrable but still chaotic on a very small scale, see [Sanders *et al.*, 2007] for references. We consider a near-integrable case ( $\varepsilon = 0.05$ ) and a chaotic case ( $\varepsilon = 1.5$ ) for system (12). The energy manifold of system (12) is compact for energy values  $0 \leq E < H_c$  with  $H_c = 1/(2\varepsilon^2)$ . In the chaotic case  $\varepsilon = 1.5$ , we have  $E = 0.1925$ ,  $H_c = 0.2222$ .

In the near-integrable case, the recurrence takes for Euclidean distance  $d = 0.1$  an interval of time around 300, in the chaotic case most tori have been



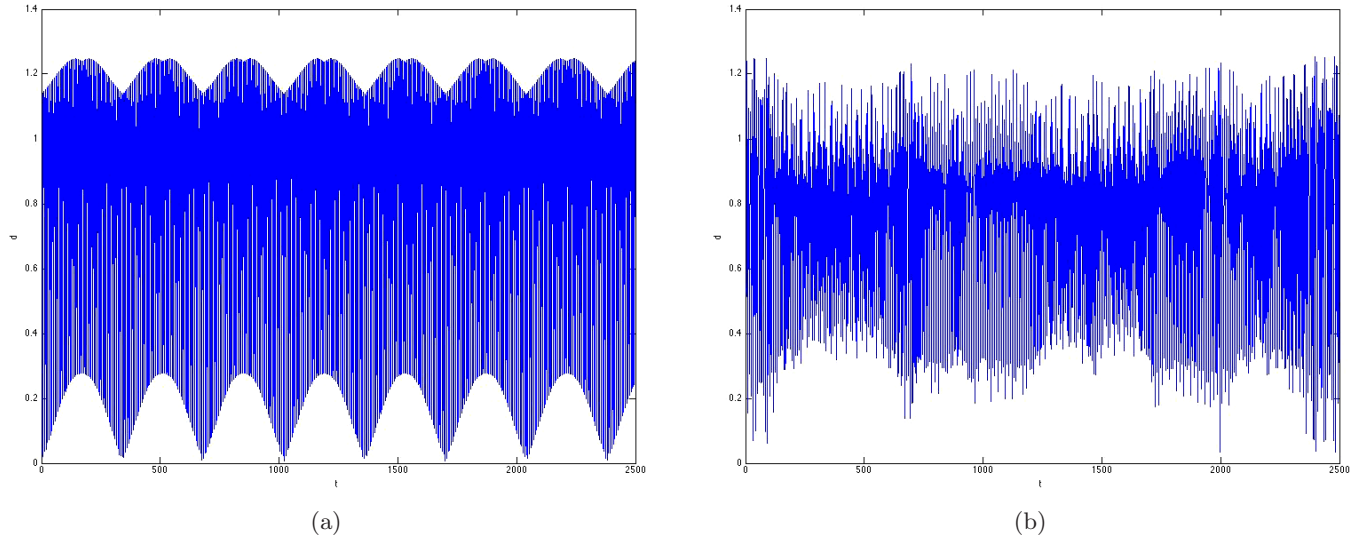


Fig. 2. The Euclidean distance for system (12) with initial conditions  $q_1(0) = 0.3$ ,  $\dot{q}_1(0) = 0$ ,  $q_2(0) = 0.5$ ,  $\dot{q}_2(0) = 0$ . (a) The near-integrable case  $\varepsilon = 0.05$  and (b) the chaotic case  $\varepsilon = 1.5$ .

destroyed and we have to integrate till  $t = 2500$  to find recurrence, see Fig. 2.

The stable solutions in one FPU-cell with four particles and so 3 dof after reduction, are surrounded by 2-tori or 3-tori (dimension 3). The energy manifold near stable equilibrium is five-dimensional ( $S^5$ ) which means that even the 3-tori do not separate  $S^5$  in phase-space. The implication is that the solutions between the tori can move off into phase-space, they are only to some extent restricted by invariant manifolds. This is sometimes called Arnold-diffusion but we will not use this term as it is not specific enough, there are different forms of diffusion in Hamiltonian systems. An increase of dimension by connecting two cells strengthens diffusion. For two cells we have eight particles and after reduction 7 dof or phase-space dimension 14. The energy manifold is  $S^{13}$  with at most tori of dimension 7, there is no separation at all.

If the normal form of the system is integrable as is the case for the classical FPU-cell, this reduces diffusion as approximate integral manifolds are present. In the case of the chaotic 3 : 2 : 1 resonance which contains horseshoe dynamics and an infinite number of close unstable periodic solutions on the energy manifold, longer recurrence times can be expected.

## (2) Quasi-trapping in resonance zones

Quasi-trapping is qualitatively discussed in [Zaslavsky, 2007]. Near stable equilibrium there

exist periodic solutions with many different periods; the stable ones are associated with invariant tori that exist in resonance zones. The solutions starting outside such a zone cannot be trapped in such a zone because of the recurrence theorem but its passage can take long intervals of time; we call this quasi-trapping. This phenomenon explains to some extent the much longer recurrence times obtained for a number of systems.

## 4. Example: The 1 : 2 : 5 Resonance

This resonance is typical for the case that the normal form to first order ( $H_3$ ) is integrable and that the next order changes the dynamics qualitatively. Its normal form was analyzed to  $H_5$  in [Van der Aa & De Winkel, 1994]; there exist four or six families of short-periodic solutions depending on the parameters and no general position short-periodic orbits. The normal form  $H_2 + \varepsilon \bar{H}_3$  is integrable. In [Haller & Wiggins, 1996], the analysis was brought to a large step further by analyzing the geometry of the perturbed integrable structure proving the existence of 3-tori and whiskered 2-tori with nearby chaotic dynamics. These phenomena have to appear as  $O(\varepsilon^2)$  effects. As in this resonance case, various timescales play a part, we consider it again from the point of view of recurrence. We restrict ourselves to potential problems as this saves parameters while keeping most of the qualitative phenomena.

In the description of tori one uses often action-angle coordinates  $I = (I, \dots, I_n)$ ,  $\phi = (\phi_1, \dots, \phi_n)$

given by:

$$p_i = \sqrt{2I_i} \cos \phi_i, \quad q_i = \sqrt{2I_i} \sin \phi_i, \quad i = 1, 2, \dots, n. \quad (13)$$

The normal form of the  $1 : 2 : 5$  resonance to  $H_4$  will contain the actions  $I_1, I_2, I_3$  and two combination angles,  $\chi_1 = 2\phi_1 - \phi_2$  and  $\chi_2 = \phi_3 - 2\phi_2 - \phi_1$ ;  $\varepsilon \bar{H}_3$  will depend on  $I_1, I_2, \chi_1$ , while adding to the normal form  $\varepsilon^2 \bar{H}_4$  we find it depends on the variables  $I_1, I_2, I_3, \chi_2$ . From Van der Aa and De Winkel [1994] we have (with constants  $a_1, b_1, \dots, b_7$ ) for the Hamiltonian normal forms:

$$\begin{cases} H_2 = I_1 + 2I_2 + 5I_3, \\ \bar{H}_3 = 2a_1 I_1 \sqrt{2I_2} \cos \chi_1, \\ \bar{H}_4 = 4(b_1 I_1^2 + b_2 I_1 I_2 + b_3 I_1 I_3 + b_4 I_2^2 \\ \quad + b_5 I_2 I_3 + b_6 I_3^2 + b_7 I_2 \sqrt{I_1 I_3} \cos \chi_2). \end{cases} \quad (14)$$

The normal form equations of motion based on system (14) are:

$$\begin{cases} \dot{I}_1 = 4\varepsilon a_1 I_1 \sqrt{2I_2} \sin \chi_1 \\ \quad - 4\varepsilon^2 b_7 I_2 \sqrt{I_1 I_3} \sin \chi_2 + \varepsilon^3 \dots, \\ \dot{I}_2 = -2\varepsilon a_1 I_1 \sqrt{2I_2} \sin \chi_1 \\ \quad - 8\varepsilon^2 b_7 I_2 \sqrt{I_1 I_3} \sin \chi_2 + \varepsilon^3 \dots, \\ \dot{I}_3 = 4\varepsilon^2 b_7 I_2 \sqrt{I_1 I_3} \sin \chi_2 + \varepsilon^3 \dots, \\ \dot{\chi}_1 = \varepsilon \frac{\sqrt{2}a_1}{\sqrt{I_2}} (4I_2 - I_1) \cos \chi_1 + \varepsilon^2 \dots, \\ \dot{\chi}_2 = -\varepsilon \frac{2\sqrt{2}a_1}{\sqrt{I_2}} (I_2 + I_1) \cos \chi_1 + \varepsilon^2 \dots. \end{cases} \quad (15)$$

The  $O(\varepsilon^2)$  terms of the equations for  $\chi_1, \chi_2$  contain  $\cos \chi_2$  but not  $\chi_1$ . Short-periodic solutions correspond with constant actions and constant combination angles  $(\chi_1, \chi_2)$ . For the normal form  $H_2 + \varepsilon \bar{H}_3$  the periodic solutions and invariant manifolds  $\text{IM}_1$  and  $\text{IM}_2$  are displayed in Fig. 3(a). Using system (15) they are described by respectively:

$$I_1 = 0, \quad I_2 = I_2(0), \quad I_3 = I_3(0), \quad (\text{IM}_1)$$

and

$$I_1 = 4I_2, \quad I_3 = I_3(0), \quad (\text{IM}_2).$$

Note that in the case of vanishing action, as in the case of  $\text{IM}_1$ , for the analysis, the normal form (14) should be replaced by an expression in

comoving coordinates. The invariant manifolds  $\text{IM}_1$  and  $\text{IM}_2$  of the normal form  $H_2 + \varepsilon \bar{H}_3$  are nonhyperbolic slow manifolds of the system generated by the normal form  $H_2 + \varepsilon \bar{H}_3 + \varepsilon^2 \bar{H}_4$ . They do not persist under the perturbation  $O(\varepsilon^2)$  as shown in Fig. 3(b). These manifolds break up with a few periodic solutions persisting whereas an intricate analysis in [Haller & Wiggins, 1996] shows the presence of horseshoe maps and chaotic dynamics at  $O(\varepsilon^2)$  level. We can analyze the behavior of the solutions in a boundary layer near  $\text{IM}_1$  by rescaling  $I_1 \rightarrow \varepsilon I_1$ . The resulting dynamics (of which we omit the details) is that in this boundary layer,  $I_2$  and  $I_3$  remain bounded while the first degree of freedom becomes parametrically excited, forcing escape from the boundary layer. This agrees with the stability analysis of Van der Aa and De Winkel [1994].

We summarize the results for the Hamiltonian  $1 : 2 : 5$  resonance without additional assumptions:

- On the right-hand side of the simplex, at  $I_1 = 0$ , we find unstable periodic solutions. Near  $\text{IM}_1$  we have the possibility of homoclinic and heteroclinic tangles as described in [Haller & Wiggins, 1996], so this part of phase-space will be our focus of attention.
- The normal form  $H_2 + \bar{H}_3$  is integrable with accuracy  $O(\varepsilon)$  and validity for all time for the integrals  $H_2$  and  $H_2 + \bar{H}_3$ ; we have the third integral  $I_3$  with accuracy  $O(\varepsilon)$  and validity on the timescale  $1/\varepsilon$ . So to  $O(\varepsilon)$  the dynamics in phase-space is dominated by the  $1 : 2$  resonance (see [Van der Aa & De Winkel, 1994]).
- Without additional assumptions, the normal form  $H_2 + \bar{H}_3 + \varepsilon^2 \bar{H}_4$  is not integrable, see [Haller & Wiggins, 1996].
- The solutions induced by the normal form (14) are describing the flow of the original Hamiltonian with accuracy  $O(\varepsilon^2)$  on the timescale  $1/\varepsilon$ .
- The recurrence times will depend on the initial conditions and also on the choice of  $\varepsilon \ll d$  [ $d$  from (9)] or  $d \ll \varepsilon$ ; the third degree of freedom may come into play especially near  $\text{IM}_1$ .

#### 4.1. Numerical experiments for the $1 : 2 : 5$ resonance

We will study recurrence behavior for a Hamiltonian that is typical for the general case discussed above; this is followed by recurrence in a FPU-cell with the same  $(1 : 2 : 5)$  resonance. It turns out that the numerics of the normal forms produce  $O(\varepsilon)$

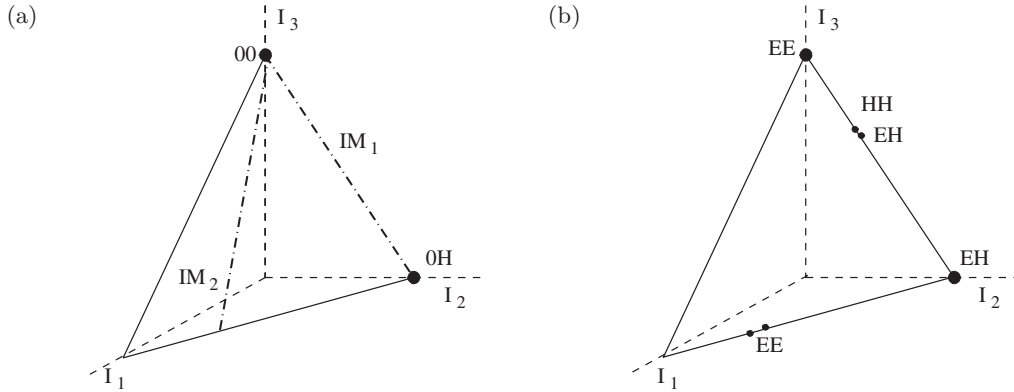


Fig. 3. The energy simplex for the Hamiltonian 1 : 2 : 5 resonance. Short-periodic solutions on the energy manifold are indicated by black dots. The small black dots on the right sides of each simplex correspond with short-periodic solutions with identical actions but different phase. The (in)stability characteristics are indicated by  $H$  (two real eigenvalues),  $E$  (two imaginary eigenvalues) and  $0$  (zero eigenvalues). The actions are displayed in the front triangle, the angles have been omitted to keep the figure three-dimensional. (a) The simplex is based on the dynamics of  $H_2 + \bar{H}_3$ , the invariant manifolds  $IM_1$  and  $IM_2$  consist of continuous families of periodic solutions and (b) the simplex based on  $H_2 + \varepsilon \bar{H}_3 + \varepsilon^2 \bar{H}_4$ , the continuous families have broken up.

precision of  $H_2$  as predicted by the theory. As an additional check of numerical accuracy we have calculated the energy given by the Hamiltonian which yields even better precision.

### An example of the general case

We choose as a typical case:

$$H_3 = -q_1^2 q_2, \quad H_4 = -\frac{5}{2} q_1 q_2^2 q_3 - \frac{1}{2} q_2^4 - q_3^4. \quad (16)$$

The equations of motion in quasi-harmonic form become:

$$\begin{cases} \ddot{q}_1 + q_1 = 2\varepsilon q_1 q_2 + \frac{5}{2} \varepsilon^2 q_2^2 q_3, \\ \ddot{q}_2 + 4q_2 = \varepsilon q_1^2 + \varepsilon^2 (5q_1 q_2 q_3 + 2q_2^3), \\ \ddot{q}_3 + 25q_3 = \varepsilon^2 \left( \frac{5}{2} q_1 q_2^2 + 4q_3^3 \right). \end{cases} \quad (17)$$

The Hamiltonian is intermediate in the sense that its terms still have to be transformed by the normalization but all of them survive the averaging-normalization process. Apart from the two normal modes we have two stable periodic solutions near  $q_3(t) = \dot{q}_3(t) = 0$  and two unstable periodic solutions near  $q_1(t) = \dot{q}_1(t) = 0$ ; see Fig. 3.

The location of the periodic solutions will guide our choice of initial conditions. We start, see Fig. 4, in general position not too far from stable periodic solutions where the 1 : 2 resonance dominates. As indicated in the caption, the recurrence time

decreases with increasing  $\varepsilon$ , a phenomenon that is typical for the near-integrable 1 : 2 resonance. It turns out that near these stable periodic solutions,  $I_3$ , which is an integral of the first order normal form valid on the time interval  $O(1/\varepsilon)$  is clearly approximately conserved in this part of phase-space for much longer times.

Starting near the  $q_2$  normal mode we find similar results with  $I(0) = 0.5$  and  $I_3(t)$  varying between 0.35 and 0.55 ( $\varepsilon = 0.2$  or  $0.3$ ), so it might be more interesting to start with larger values of  $q_3$ .

Near the  $I_1 = 0$  side on the simplex of Fig. 3 we choose the initial values  $q_1(0) = 0.04$ ,  $q_2(0) = 0.4$ ,  $q_3(0) = 0.3683$ . As before the recurrence times become shorter with increasing  $\varepsilon$ ; see Fig. 5.

However, the variations of the actions present a surprise. Consider Fig. 6 where  $I_3(t)$  and  $H_2$  are displayed for  $\varepsilon = 0.1, 0.2, 0.3$  (from left to right on the same scale 0–2.5). For  $\varepsilon = 0.1$  the variation of the action  $I_3$  is  $O(\varepsilon)$ ; this can be understood from Fig. 5 where the recurrence clearly takes a longer time than  $t = 10000$ . For  $\varepsilon = 0.3$  [Fig. 6(c)] the variation is clearly larger, but remarkably enough, it is much larger for  $\varepsilon = 0.2$  (between 0.2 and 1.7). For comparison we display also the behavior of  $I_1(t)$  and  $H_2(t)$ . This shows that near the unstable periodic solutions starting for a small value of  $I_1$ , we experience fast and strong oscillations of  $I_1(t)$ . These variations can be associated with the homoclinic and heteroclinic tangles resulting in chaotic behavior in small subsets as predicted in [Haller & Wiggins, 1996].



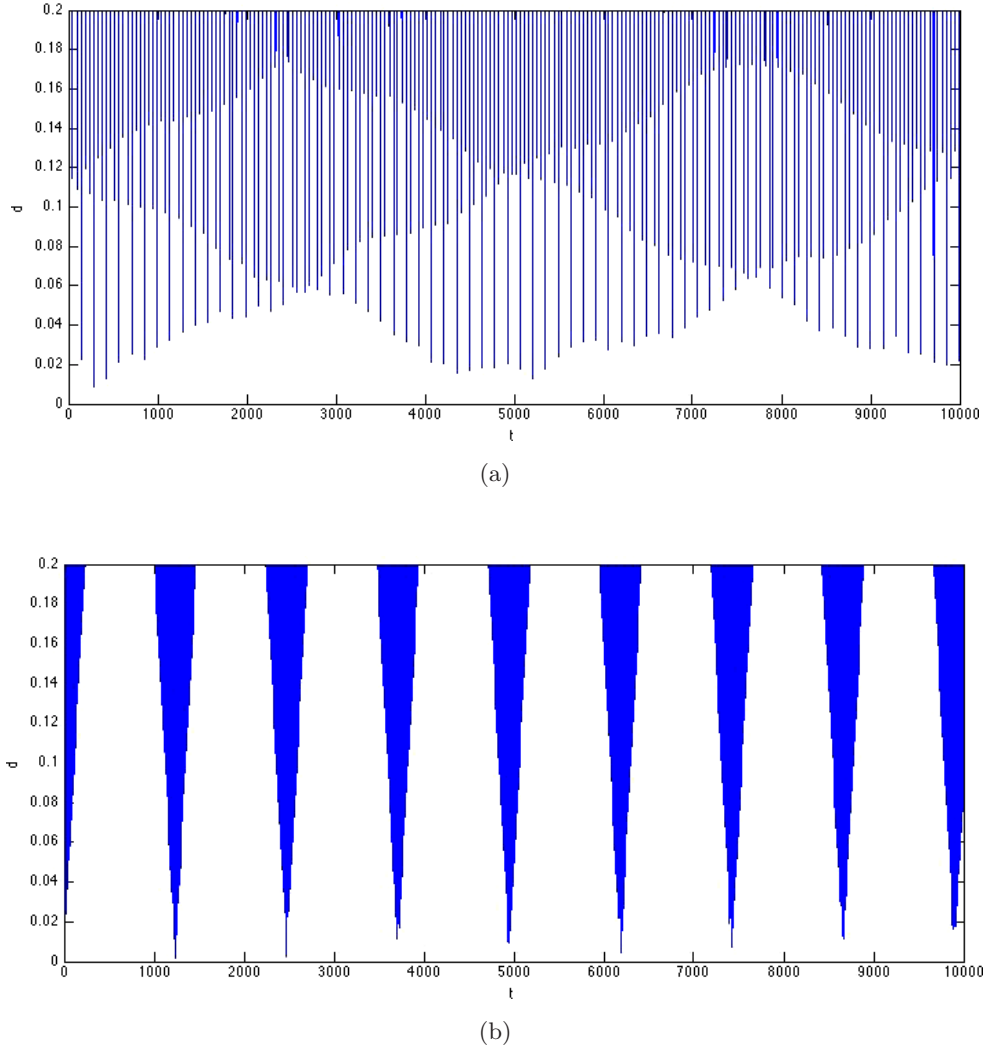


Fig. 4. The recurrence distance (9) with time  $0 \leq t \leq 10\,000$  based on system (17) when starting not far from the stable periodic solutions on the  $I_3 = 0$  side of Fig. 3 of the Hamiltonian  $1 : 2 : 5$  resonance;  $q_1(0) = 1.4$ ,  $q_2(0) = 0.5$ ,  $q_3(0) = 0.2$ . (a) The case  $\varepsilon = 0.1$  and (b)  $\varepsilon = 0.3$ ;  $E_0 = 1.98$ . The recurrence time decreases if  $\varepsilon$  increases;  $I_3(0) = 0.5$ ,  $I_3(t)$  varies for  $\varepsilon = 0.1$  (a) between 0.481 and 0.5, for  $\varepsilon = 0.3$  and (b) between 0.435 and 0.5.

#### 4.1.1. The FPU $1 : 2 : 5$ resonance

Inspired by [Bruggeman & Verhulst, 2015, Table 1], we will study a FPU-cell from system (3) with inverse masses:

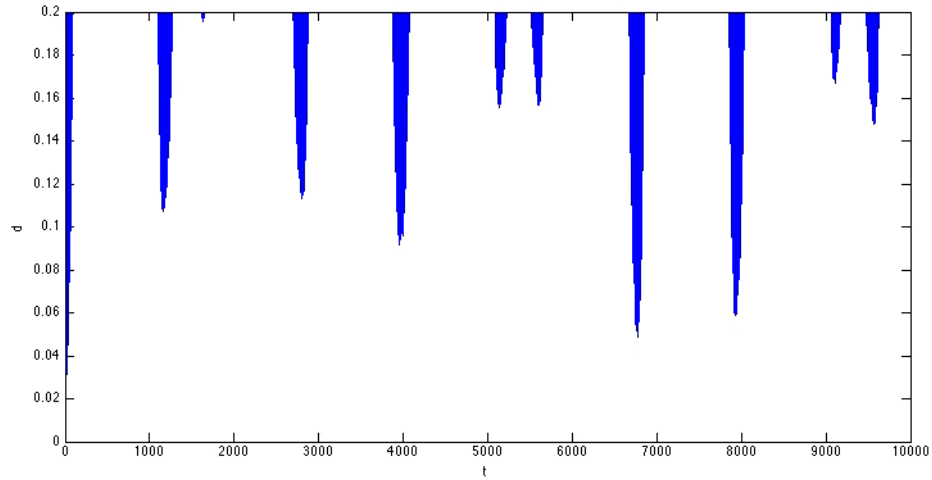
$$\begin{aligned} a_1 &= 0.00587407, & a_2 &= 0.0213455, \\ a_3 &= 0.0813377, & a_4 &= 0.391443. \end{aligned} \quad (18)$$

The (inverse) masses were chosen in an open parameter subset characterized by qualitatively similar dynamics so this choice is typical. As the  $a_1, \dots, a_4$  are fairly small, we will take  $\varepsilon$  around or at 0.5 as this produces already small right-hand sides in system (3). It turns out that starting near particles one, three or four in the FPU-cell, the recurrence

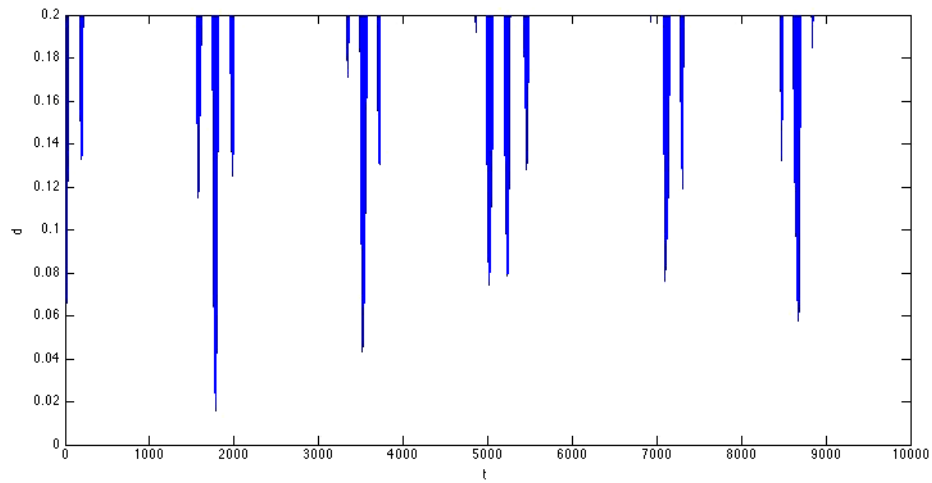
is quite similar [Fig. 8(a)]; however, starting near particle two the recurrence is delayed, see Fig. 8(b).

The numerical results of Fig. 8 suggest that the dynamics of the FPU-cell is similar to the behavior of the general  $1 : 2 : 5$  resonance described above in this subsection. To check this conjecture we perform a symplectic transformation to reduce the four-dimensional FPU-cell to a three-dimensional system using the momentum integral; see for the procedure [Bruggeman & Verhulst, 2015]. With the choice of masses (18) we find in the notation of Bruggeman and Verhulst [2015]:

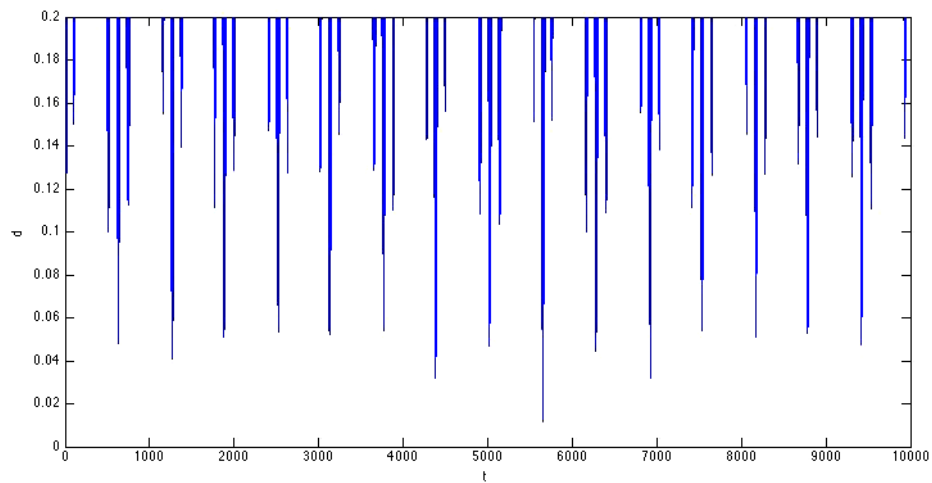
$$H_2(x, y) = \frac{1}{2} \sum_{i=1}^3 (y_i^2 + \omega_i^2 x_i^2),$$



(a)



(b)



(c)

Fig. 5. The recurrence distance (9) with time  $0 \leq t \leq 10\,000$  based on system (17) when starting near the  $I_1 = 0$  side of Fig. 3 of the Hamiltonian  $1 : 2 : 5$  resonance;  $q_1(0) = 0.04$ ,  $q_2(0) = 0.4$ ,  $q_3(0) = 0.3683$ ,  $H_2(0) = 1.98$ . From (a) to (c) we have  $\varepsilon = 0.1, 0.2, 0.3$ . The recurrence time decreases with increasing  $\varepsilon$  as expected.

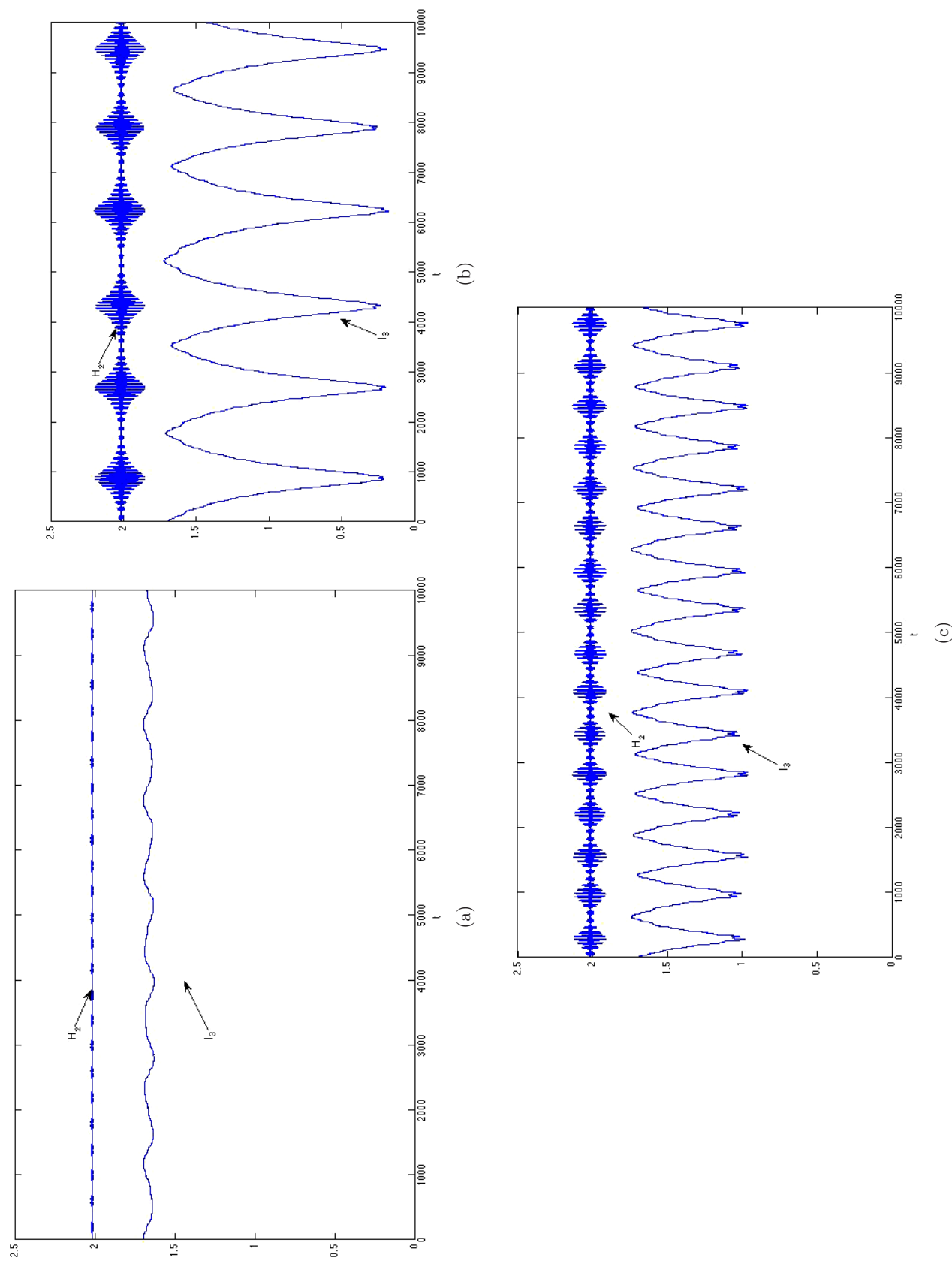


Fig. 6. The variations of  $H_2$  and  $I_3$  with time  $0 \leq t \leq 10\,000$  based on system (17) when starting near the  $I_1 = 0$  side of Fig. 3 of the Hamiltonian 1 : 2 : 5 resonance;  $q_1(0) = 0.04$ ,  $q_2(0) = 0.4$ ,  $q_3(0) = 0.3683$ ,  $H_2(0) = 1.98$ . From (a) to (c) we have  $\varepsilon = 0.1, 0.2, 0.3$ , the variations of  $I_3(t)$  are respectively between 1.63 and 1.7, between 0.2 and 1.7 and between 1 and 1.75.

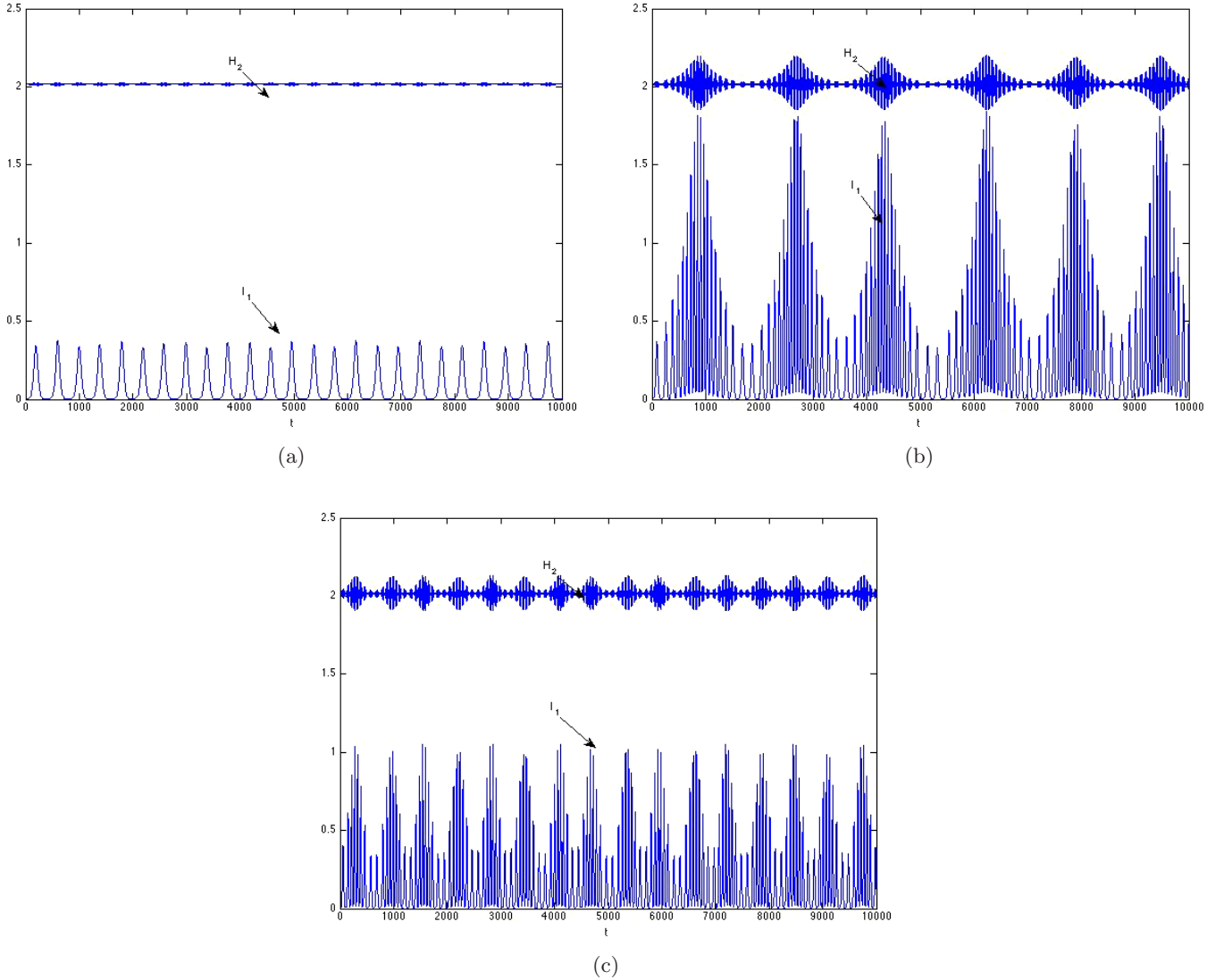


Fig. 7. The variations of  $H_2$  and  $I_1$  with time  $0 \leq t \leq 10\,000$  based on system (17) with the same data as in Fig. 6. From (a) to (c) we have  $\varepsilon = 0.1, 0.2, 0.3$ , the variations of  $I_1(t)$  are of much higher frequency than of  $I_3(t)$ , especially for  $\varepsilon = 0.2$ .

with

$$\omega_1^2 = 0.0333334, \quad \omega_2^2 = 0.1333334, \\ \omega_3^2 = 0.833334.$$

The calculation for  $H_3$  produces:

$$\left\{ \begin{array}{l} H_3 = -0.00107405x_1^3 + 0.00216916x_1^2x_2 \\ \quad + 0.000202739x_1^2x_3 + 0.00432288x_1x_2^2 \\ \quad - 0.00231034x_1x_2x_3 + 0.0535357x_1x_3^2 \\ \quad - 0.00833532x_2^3 - 0.0144427x_2^2x_3 \\ \quad + 0.102058x_2x_3^2 + 0.0283995x_3^3. \end{array} \right. \quad (19)$$

The equations of motion will be compared with system (17) of the general case so we replace positions

$x$  by  $q$  and rescale time to obtain:

$$\left\{ \begin{array}{l} \ddot{q}_1 + q_1 = \varepsilon(0.096664q_1^2 - 0.260299q_1q_2 \\ \quad - 0.012164q_1q_3 - 0.129686q_2^2 \\ \quad + 0.069310q_2q_3 - 1.606068q_3^2), \\ \ddot{q}_2 + 4q_2 = \varepsilon(-0.065075q_1^2 - 0.259372q_1q_2 \\ \quad + 0.069310q_1q_3 + 0.750177q_2^2 \\ \quad + 0.866560q_2q_3 - 3.061734q_3^2), \\ \ddot{q}_3 + 25q_3 = \varepsilon(-0.006082q_1^2 + 0.069310q_1q_2 \\ \quad - 3.212136q_1q_3 + 0.433280q_2^2 \\ \quad - 6.123468q_2q_3 - 2.555950q_3^2). \end{array} \right. \quad (20)$$

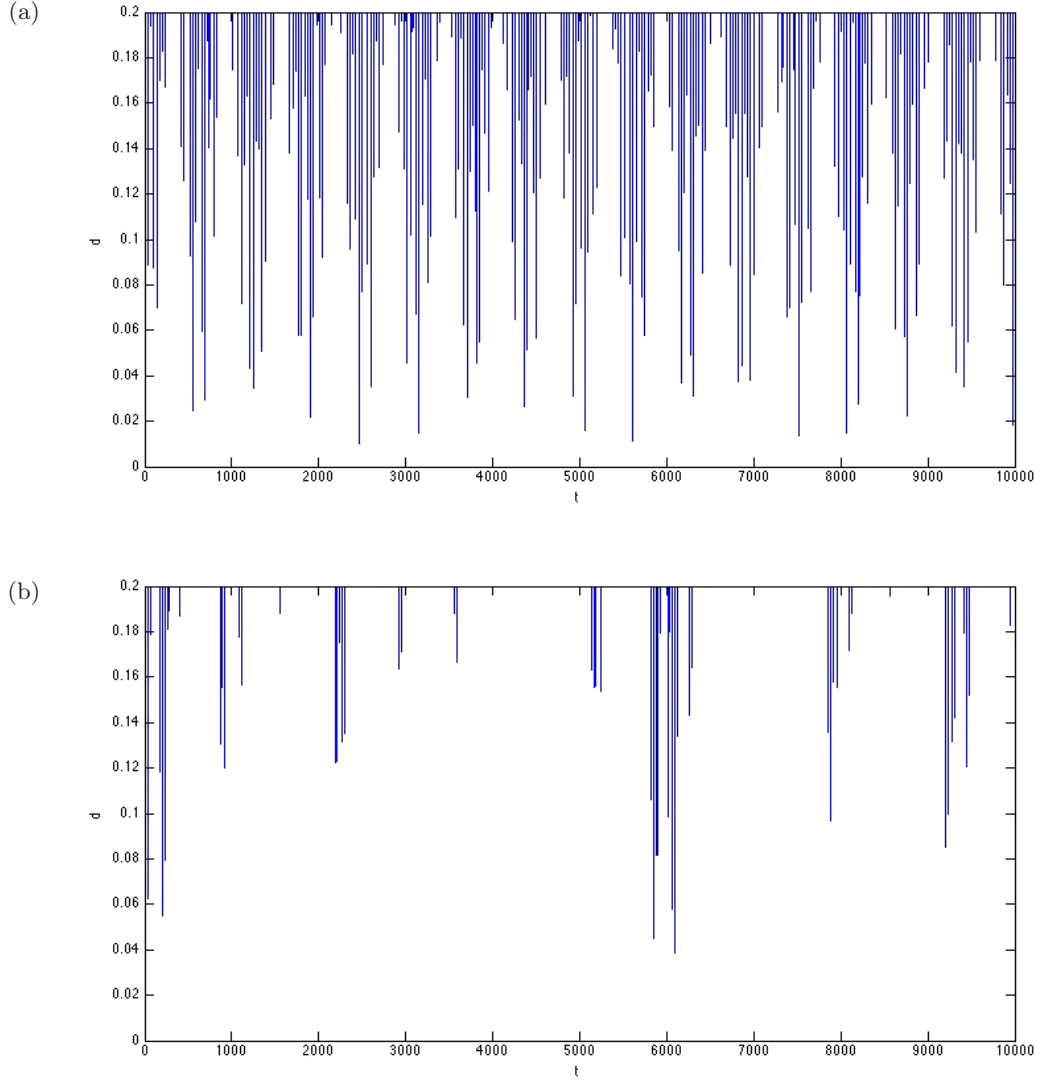


Fig. 8. The recurrence distance (9) with time  $0 \leq t \leq 10\,000$  when starting in a FPU-cell described by system (3) near (a) the fourth particle and (b) the second one. We have chosen (a)  $\varepsilon = 0.5$ ,  $q_1(0) = 0.1$ ,  $q_2(0) = -0.1$ ,  $q_3(0) = 0.15$ ,  $q_4(0) = 1$  and (b)  $q_1(0) = 0.1$ ,  $q_2(0) = 1$ ,  $q_3(0) = -0.1$ ,  $q_4(0) = 0.15$ .

As we have seen in system (14), normalization of  $H_3$  leaves only the term  $q_1^2 q_2$  in  $\bar{H}_3$ . We checked that normalizing to  $\bar{H}_4$  of the FPU  $H_3$  given in (19) produces interaction with the third degree of freedom as in the general case of system (14); we will not present the full calculation of  $\bar{H}_4$  but restrict ourselves to a few illustrations. Based on system (20) we start near the  $I_1 = 0$  side of the simplex of Fig. 3. The recurrence as shown in Fig. 9 has been delayed.

The action  $I_3$  and the normal form integral  $H_2$  of this case are shown in Fig. 10. Remarkably enough  $I_3(t)$  varies with  $O(\varepsilon)$  far beyond its interval of validity but it still represents a drift away from the dominating 1 : 2 resonance of the first two

modes; see the note on quasi-trapping in Sec. 3.3. Repeating the integration near the  $I_3$  normal mode shows stable behavior as expected from the simplex in Fig. 3.

For reasons of comparison we also consider initial conditions in general position directly in system (7) with the 1 : 2 : 3 resonance condition from (18). The Euclidean distance  $d$  for one and two cells are shown in Fig. 11. For the chosen initial conditions the recurrence in one cell is fairly good, linking to a second cell we have larger and more frequent fluctuations of  $d$ .

A remarkable feature is that the action  $I_3$  varies again very little and that the recurrence when starting near  $I_1 = 0$  as in Fig. 9 takes much longer than



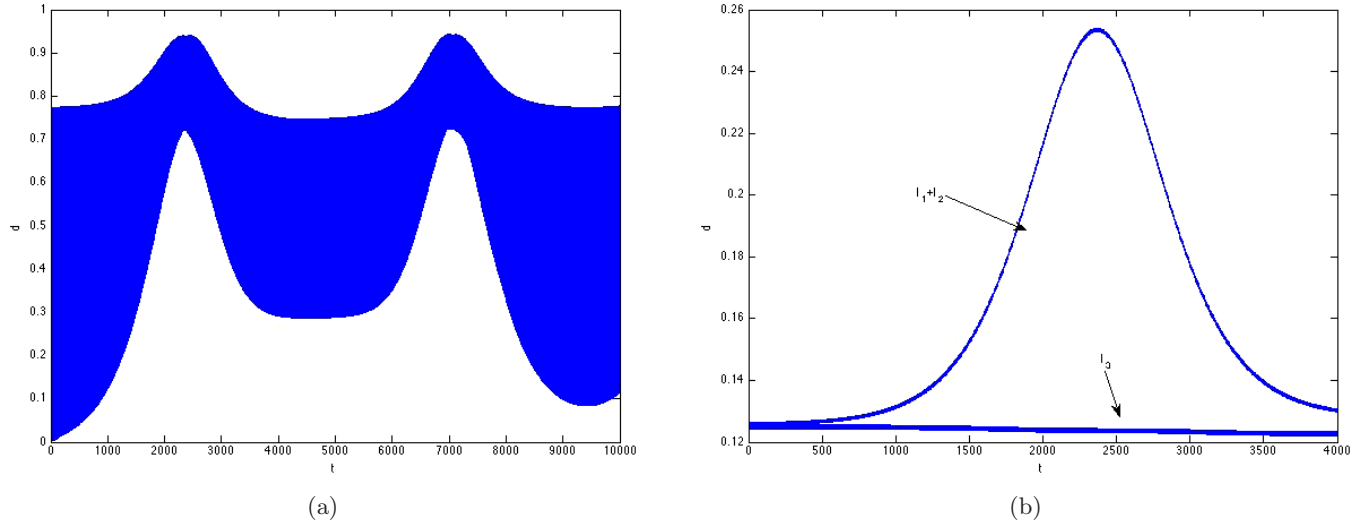


Fig. 9. (a) The recurrence distance (9) with time  $0 \leq t \leq 10\,000$  when starting in a FPU-cell described by system (20) near the action  $I_1 = 0$ . We have chosen  $\varepsilon = 0.1$ ,  $q_1(0) = 0.04$ ,  $q_2(0) = 0.25$ ,  $q_3(0) = 0.1$ . The recurrence takes place near  $t = 10\,000$  but is far from complete; compare also the recurrence in the 2 dof 1 : 2 resonance for which distance  $d$  is shown in Fig. 2. (b) For  $0 \leq t \leq 4000$  the behavior of the actions  $I_1 + I_2$  which are in primary resonance 1 : 2 whereas as a secondary effect the action  $I_3$  feeds energy into the 1 : 2 resonance causing a drift in phase-space.

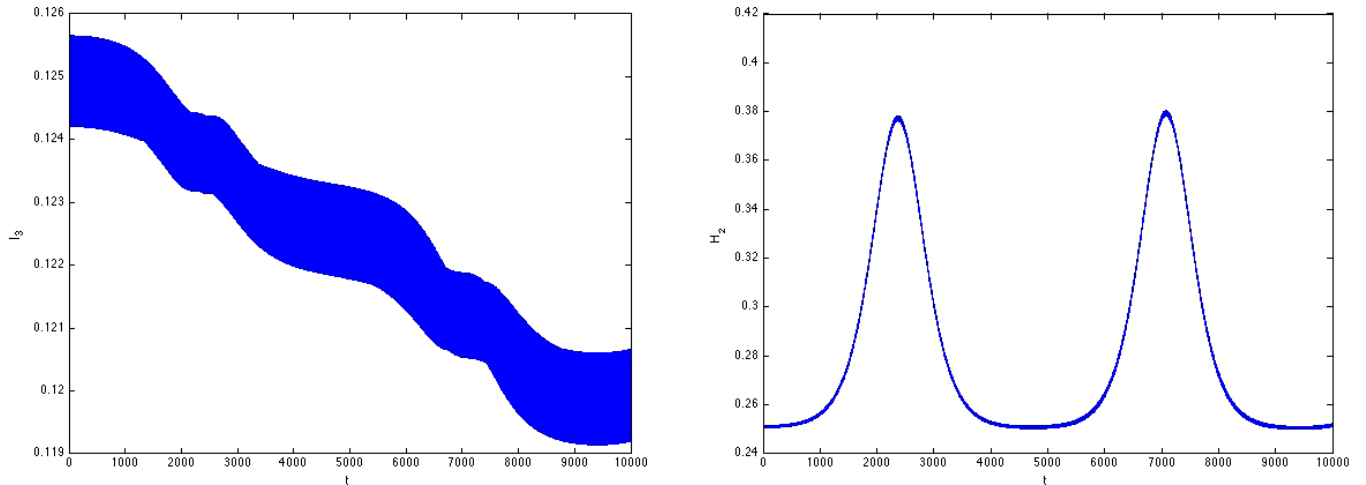


Fig. 10. Time series for the action  $I_3$  and for  $H_2$  with time  $0 \leq t \leq 10\,000$  when starting in a FPU-cell described by system (20) near the action  $I_1 = 0$ .  $\varepsilon = 0.1$ , the initial conditions are as in Fig. 9.  $I_3(0) = 0.125$  and  $I_3$  varies between 0.119 and 0.126 (far beyond its interval of validity);  $E_0 = 0.251$ ,  $H_2$  varies between 0.251 and 0.38.

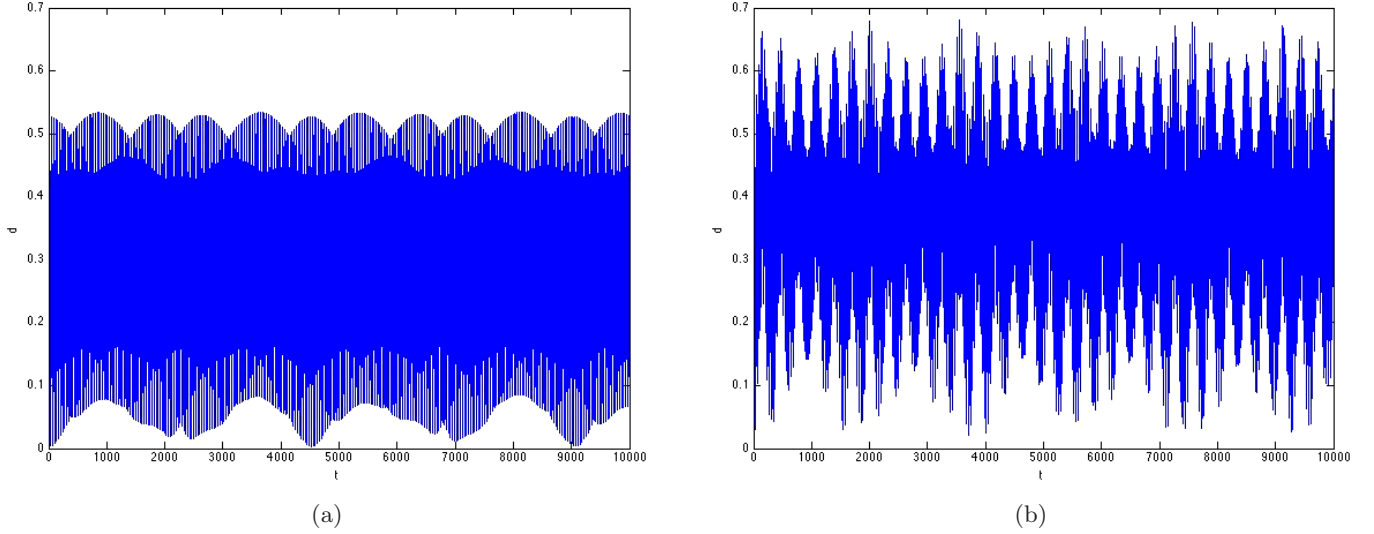


Fig. 11. The recurrence distance (9) with time  $0 \leq t \leq 10000$  when starting in a FPU-cell in  $1 : 2 : 5$  resonance described by system (7) with masses from (18). We have chosen  $\varepsilon = 0.5$  and  $q_1(0) = 0.05$ ,  $q_2(0) = 0.2$ ,  $q_3(0) = 0.1$ ,  $q_4(0) = 0.3$ , zero for the other positions and the velocities. (a) The case of one cell ( $c_1 = 0$ ) and (b) two cells ( $c_1 = 0.1$ ).

starting in general position. This can be explained by the chaos phenomena in small subsets as shown in [Haller & Wiggins, 1996] and for the  $1 : 2 : 5$  resonance as a secondary effect quasi-trapping in the form of drifting around the  $1 : 2$  resonance.

## 5. The Classical, Near-Integrable FPU Case of Equal Masses

The normal form used in this section for one cell was derived in [Rink & Verhulst, 2000] (Sec. 4.2). Inspection of system (3) shows that three exact periodic solutions exist corresponding with normal modes (motion restricted to 1 dof) in the classical case ( $a_i = 1$ ). As we shall see, using the normal form, the symmetry of system (3) produces four quasi-periodic families of solutions in general position (away from the normal modes). So, the classical case has in addition four families of stable quasi-periodic solutions with basic frequencies  $\sqrt{2}, 2, \sqrt{2}$ .

### 5.1. The phase-flow in one cell

Considering one cell, one can reduce the number of dof to three by using the momentum integral (4). Using a suitable symplectic transformation system (3) as in [Bruggeman & Verhulst, 2015] we find with  $a_i = 1$  the symmetric-looking system:

$$\begin{cases} \ddot{x}_1 + 2x_1 = 4\varepsilon x_2 x_3, \\ \ddot{x}_2 + 4x_2 = 4\varepsilon x_1 x_3, \\ \ddot{x}_3 + 2x_3 = 4\varepsilon x_1 x_2. \end{cases} \quad (21)$$

An important difference with the  $1 : 2 : 5$  resonance is that in this case the integrable structure of the  $1 : 1$  resonance is not resonantly perturbed by the higher order normal forms. The normal modes described above are now found as harmonic functions on the coordinate axes. It is also clear (because

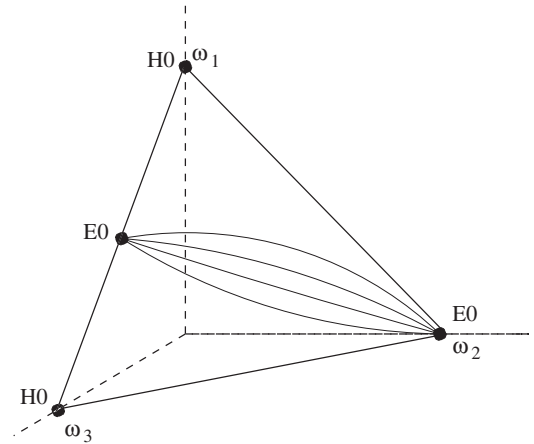


Fig. 12. The energy simplex for the classical FPU-cell;  $\omega_1 = \sqrt{2}$ ,  $\omega_2 = 2$ ,  $\omega_3 = \sqrt{2}$ . Short-periodic solutions on the energy manifold are indicated by black dots. The (in)stability is indicated by  $H$  (two real eigenvalues),  $E$  (two imaginary eigenvalues) and  $0$  (zero eigenvalues). The actions are displayed in the front triangle, the angles have been omitted to keep the figure three-dimensional. The  $\omega_2$  normal mode is stable, the  $\omega_1$  and  $\omega_3$  normal modes are unstable with two real eigenvalues. At  $I_2 = 0$  there are four stable short-periodic solutions, the curves connecting these four solutions with the  $\omega_2$  normal mode represent four families of quasi-periodic solutions.

of the symmetry) that  $x_1(t) = \pm x_3(t)$  satisfies system (21).

Normalization of system (21) produces more details of the flow. In action-angle coordinates  $(I, \psi)$  with as usual  $dI/dt = -\partial H/\partial \psi$ ,  $d\psi/dt = \partial H/\partial I$  the expression for  $H_2$  is:

$$H_2 = \sqrt{2}I_1 + 2I_2 + \sqrt{2}I_3.$$

We have  $\bar{H}_3 = 0$ ,  $\bar{H}_4$  is nontrivial. In action-angle coordinates the normal form becomes  $O(\varepsilon^2)$ :

$$\begin{aligned} H_2 + \bar{H}_4 &= \sqrt{2}I_1 + 2I_2 + \sqrt{2}I_3 - \frac{\varepsilon^2}{2}I_1I_3 \cos 2\chi \\ &+ \frac{1}{2}\varepsilon^2\sqrt{2}I_2(I_1 + I_3), \quad \chi = \psi_1 - \psi_3. \end{aligned} \quad (22)$$

The phase-flow of system (3) in the classical case is approximated to  $O(\varepsilon)$  on the timescale  $1/\varepsilon^2$  by the flow of the normal form. The discussion and approximation of the normalized flow follows the reasoning of Sanders *et al.* [2007] and Verhulst [2015a]. In action-angle coordinates and truncated at  $O(\varepsilon^3)$ , the normalized equations of motion are:

$$\begin{cases} \frac{dI_1}{dt} = -\varepsilon^2 I_1 I_3 \sin 2\chi, \\ \frac{d\psi_1}{dt} = \sqrt{2} - \frac{\varepsilon^2}{2}(I_3 \cos 2\chi - \sqrt{2}I_2), \\ \frac{dI_2}{dt} = 0, \quad \frac{d\psi_2}{dt} = 2 - \frac{1}{2}\varepsilon^2\sqrt{2}(I_1 + I_3) \\ \frac{dI_3}{dt} = \varepsilon^2 I_1 I_3 \sin 2\chi, \\ \frac{d\psi_3}{dt} = \sqrt{2} - \frac{\varepsilon^2}{2}(I_1 \cos 2\chi - \sqrt{2}I_2). \end{cases} \quad (23)$$

The normal form equations (23) are integrable with integrals  $I_1 + I_3 = E_1$ ,  $I_2 = E_2$  and  $H_2 + \bar{H}_4$  with  $E_1, E_2$  constants determined by the initial conditions. As the normalized system is integrable, the original system (3) is near-integrable in this classical case. The flow on the energy manifold (a deformation of  $S^5$ ) of the reduced system is relatively simple. The normal modes  $x_1$  and  $x_3$  are linked on  $S^5$  in 1 : 1 resonance. Starting near one of these unstable periodic solutions, the trajectory will move on a torus surrounding a stable periodic solution while  $I_2$  is constant to  $O(\varepsilon)$ ; it will then return near its starting point in a typical interval of time  $O(1/\varepsilon^2)$ ,

see also Fig. 13. The amount of chaos between the tori of the original system (3) is  $O(\varepsilon)$ .

Apart from the three normal modes we have from system (23) constant actions if  $\sin 2\chi = 0$  for  $t \geq 0$ . We have

$$\frac{d}{dt}(2\chi) = \varepsilon^2(I_1 - I_3) \cos 2\chi,$$

so these solutions exist if

$$I_1 = I_3 = \frac{1}{2}E_1, \quad \chi = 0, \quad \frac{\pi}{2}, \quad \pi, \quad \frac{3\pi}{2}, \quad (24)$$

corresponding with four periodic solutions if  $I_2 = 0$  in system (23). If  $I_2(0) > 0$  we have four continuous families of quasi-periodic solutions with frequencies near  $\sqrt{2}$  and 2 on the energy manifold. The presence of these continuous families is connected with the existence of the third integral  $I_2$  in the normal form. The four quasi-periodic families link their position in the  $I_2 = 0$  coordinate plane with the  $x_2$  (second) normal mode. When normalizing to higher order, these families of quasi-periodic solutions do not break-up for  $\varepsilon$  small enough as the frequency ratio  $\sqrt{2} : 2$  is irrational. This irrationality makes also for the stability of the quasi-periodic solutions. The results are displayed in the action-simplex of Fig. 12.

## 5.2. Numerical calculation of recurrence

When calculating the Euclidean distance (9) for one cell starting near the stable normal mode 2, choosing  $d = 0.01$  and  $E_0 = 1.2721$ , the upper bound  $L$  of the recurrence time will be  $O(10^{10})$ . However, on the interval of time  $[0, 12000]$  the distance  $d$  to the initial phase-point is 15 times smaller than 0.01. This is caused by the stability of the normal mode in this near-integrable system. In Fig. 13, we started near an unstable normal mode.

Starting near the unstable normal mode 1 in Fig. 13, the solution moves away on a torus around another, stable periodic solution. The recurrence time depends on the approximate energy  $E_0 = 0.847917$  if  $\varepsilon = 0.2$  and the distance to the unstable normal mode. The upper bound of the recurrence time is again  $O(10^{10})$  but the recurrence is much faster because of the near-integrability of the classical FPU-cell to arbitrary order (in contrast to the 1 : 2 : 5 resonance where the near-integrability breaks up at second order). Motion on the torus will

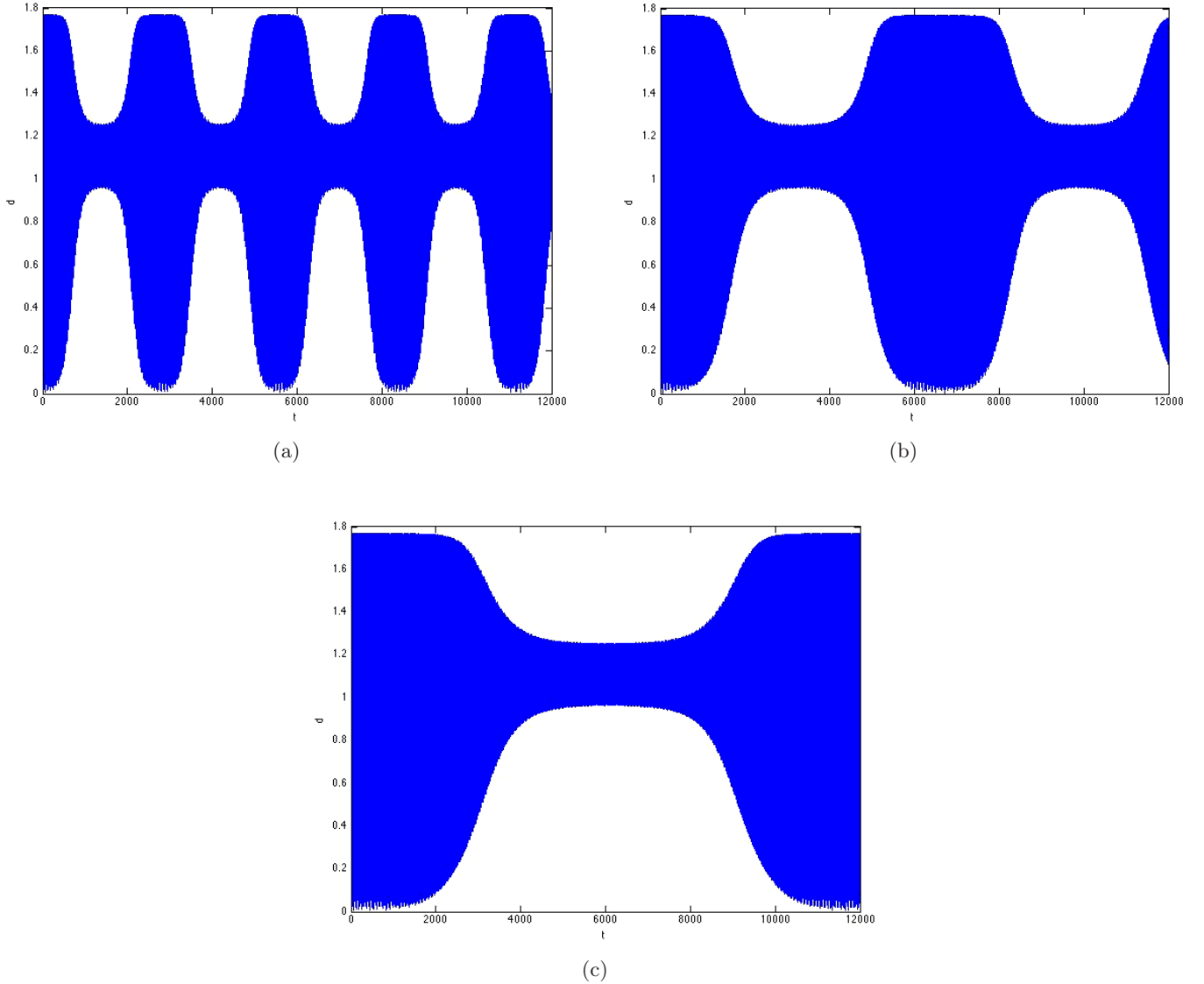


Fig. 13. The Euclidean distance  $d$ , see (9), for one cell in the classical case with initial conditions near the unstable normal mode 1:  $a_i = 0.1$ ,  $v_i(0) = 0$ ,  $i = 1, \dots, 4$ ;  $q_1(0) = 0.6$ ,  $q_2(0) = 0$ ,  $q_3(0) = -0.65$ ,  $q_4(0) = 0$ . The interval of time is  $[0, 12000]$ , the recurrence time decreases with increasing  $\varepsilon$ ; (a) the distance  $d$  is near to zero for  $t \in [2000, 2500]$  if  $\varepsilon = 0.3$ . (b) If  $\varepsilon = 0.2$  the recurrence takes place for  $t \in [6000, 7000]$ , (c) if  $\varepsilon = 0.15$  the recurrence needs  $t \in [11000, 12000]$ .

take a time interval  $O(1/\varepsilon^2)$  and the recurrence time will be proportional to a power of  $1/d$  and  $O(1/\varepsilon^2)$ , see Fig. 13. The recurrence time decreases with  $\varepsilon$  as this increases the interaction of the modes, see again Fig. 13.

### 5.3. Linking $n$ cells

As mentioned before, cells can be linked in various ways. Here, we will follow the set-up of Sec. 1 and Fig. 1, connecting  $n$  identical 4 dof cells by particles 2–6, 8–10, 12–14, etc. We start with the case of two cells.

Linking two cells ( $c_1 \neq 0$ ,  $c_2 = 0$ ) we increase the dimension and we expect longer recurrence times; see Fig. 14 where the initial energy is restricted to the first cell. We can find the following exact solutions:

- (1) The periodic solutions given by:  $q_1 + q_3 = 0$ ,  $q_5 + q_7 = 0$ ,  $\ddot{q}_i + 2q_i = 0$ ,  $i = 1, 3, 5, 7$ ,  $q_2 = q_4 = q_6 = q_8 = 0$ . Starting with this harmonic solution (frequency  $\sqrt{2}$ ) there will be no energy transfer between the cells.
- (2) The quasi-periodic solutions given by:  $q_2 + q_4 = 0$ ,  $q_6 + q_8 = 0$ ,  $q_1 = q_3 = q_5 = q_7 = 0$ ; the 4 dof subsystem has frequencies  $\sqrt{2}$ ,  $\sqrt{2(1 + \varepsilon c_1)}$ .

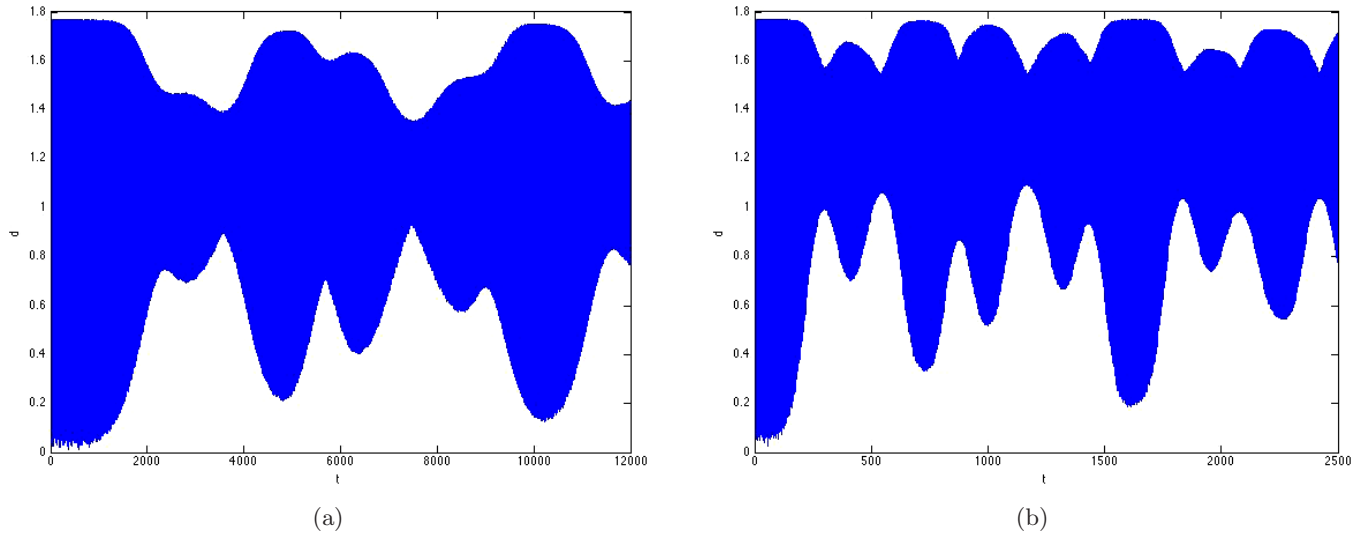


Fig. 14. The Euclidean distance (9) for two cells ( $c_1 = 0.1$ ) in the classical case with initial conditions near the unstable normal mode 1 in cell 1, zero initial energy in the second cell;  $v_i(0) = 0$ ,  $i = 1, \dots, 4$ ;  $q_1(0) = 0.6$ ,  $q_2(0) = 0$ ,  $q_3(0) = -0.65$ ,  $q_4(0) = 0$ . The interval of time is  $[0, 2500]$ , clearly the recurrence time increases as the number of dof has been increased. (a) The Euclidean distance in the case  $\varepsilon = 0.2$  and (b)  $\varepsilon = 0.3$ ; in both cases vertical scale  $[0, 1.8]$ .

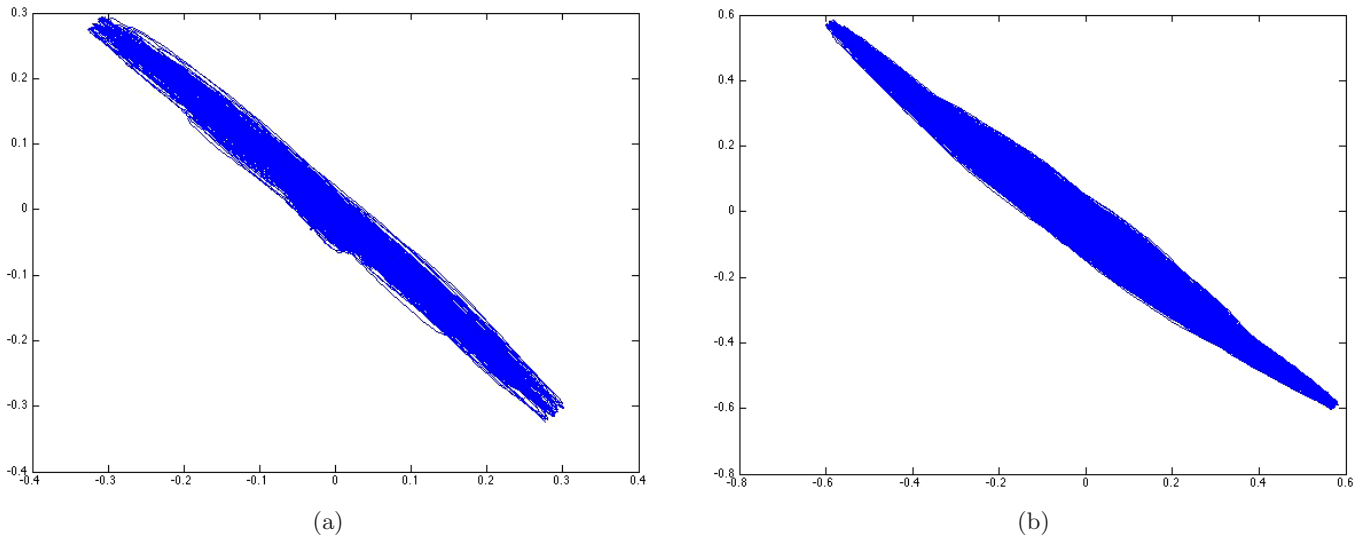


Fig. 15. The 1 : 1 resonance arising in the second cell ( $c_1 = 0.1$ ) in the classical case with initial conditions near the unstable normal mode 1 in cell 1, zero initial energy in the second cell;  $v_i(0) = 0$ ,  $i = 1, \dots, 4$ ;  $q_1(0) = 0.6$ ,  $q_2(0) = 0$ ,  $q_3(0) = -0.65$ ,  $q_4(0) = 0$ . The interval of time (a) is  $[0, 2500]$  (range  $[-0.4, 0.4]$ ) and (b)  $[0, 12500]$  (range  $[-0.6, 0.6]$ );  $\varepsilon = 0.3$ . Quasi-trapping takes longer than 12 500 time steps.



If  $q_2 = q_6$ , the solution becomes periodic but in this case there is no exchange of energy between the cells.

- (3) The quasi-periodic solution involving the 8 dof given by:  $q_1 = -q_2 = q_3 = -q_4$ ,  $q_5 = -q_6 = q_7 = -q_8$  with frequencies 2 and  $2 + O(\varepsilon)$ .

If  $q_2 = q_6$ , the solution becomes periodic but in this case there is no exchange of energy between the cells.

Consider now the case of  $n$  cells with linking as chosen above. We generalize easily to:

- (1) A  $\sqrt{2}$ -periodic solution exists under the conditions  $q_{1+i} + q_{3+i} = 0$ ,  $i = 0, 4, 8, \dots$  and all modes with even index ( $q_2, q_4, q_6, \dots$ ) zero.
- (2) A quasi-periodic solution exists with frequency  $\sqrt{2}$  and  $(n-1)$  frequencies  $\sqrt{2} + O(\varepsilon)$  if  $q_{2+i} + q_{4+i} = 0$ ,  $i = 0, 4, 8, \dots$  and all modes with odd index ( $q_1, q_3, q_5, \dots$ ) zero.
- (3) The quasi-periodic solution involving the  $4n$  dof given by:

$$\begin{aligned} q_1 &= -q_2 = q_3 = -q_4, \\ q_5 &= -q_6 = q_7 = -q_8, \dots, q_{4n-3} \\ &= -q_{4n-2} = q_{4n-1} = -q_{4n} \end{aligned}$$

with frequency 2 and  $(n-1)$  frequencies  $2 + O(\varepsilon)$ .

Under additional assumptions the solution will be periodic.

The extension of the recurrence time when using two cells is caused by quasi-trapping (Sec. 3.3). We illustrate this in Fig. 15 where we observe the interaction between  $q_5$  and  $q_7$  in the second cell. On the time interval  $[0, 2500]$  we observe behavior near a  $1 : 1$  resonance, on the interval  $[0, 12500]$   $q_5$  and  $q_7$  increase their range to  $[-0.6, 0.6]$ . The recurrence theorem guarantees that the solutions will leave this quasi-trapping region after some time.

## 6. Chaotic Cells in $3 : 2 : 1$ Resonance

As a last and very different FPU-cell we consider a chain with unequal masses leading to chaotic dynamics in the first order normal form.

### 6.1. Transformation to a quasi-harmonic form

The presence of the momentum integral enables us to reduce system (3) to a 3 dof system. It has been shown in [Bruggeman & Verhulst, 2015] that the  $\omega_1 : \omega_2 : \omega_3 = 3 : 2 : 1$  resonance arises as a one-parameter family of Hamiltonians; many other resonances can be found. Without loss of generality we choose

$$\omega_1^2 = \frac{9}{14}, \quad \omega_2^2 = \frac{4}{14}, \quad \omega_3^2 = \frac{1}{14}. \quad (25)$$

The one-parameter family of  $3 : 2 : 1$  resonances is characterized by the real parameter  $u \in [0, \bar{u}]$  with  $\bar{u} = 0.887732 \dots$ . In an application later on we will choose a particular value of  $u$ , called case 1 in [Bruggeman & Verhulst, 2015], that is typical. To put system (3) in the standard form of quasi-harmonic equations we have to apply a suitable symplectic transformation  $L(u)^{-1} : p, q \rightarrow y, x$  with  $x$  the vector of the new position variables. This leads to a transformed Hamiltonian, again of polynomial form  $H_2 + \varepsilon H_3$  with

$$H_2 = \frac{1}{2} \left( \dot{x}_1^2 + \frac{9}{14} x_1^2 + \dot{x}_2^2 + \frac{4}{14} x_2^2 + \dot{x}_3^2 + \frac{1}{14} x_3^2 \right)$$

and  $H_3$  a cubic expression containing ten terms, see for details [Bruggeman & Verhulst, 2015]. Because of the  $3 : 2 : 1$  resonance, only two terms will be active in the normalized  $H_3$ ; leaving out the eight terms that play no part in the normalized  $H_3$  we have an *intermediate normal form* of the equations of motion:

$$\begin{cases} \ddot{x}_1 + \frac{9}{14} x_1 = -\varepsilon d_6 x_2 x_3, \\ \ddot{x}_2 + \frac{4}{14} x_2 = -\varepsilon (d_6 x_1 x_3 + d_9 x_3^2), \\ \ddot{x}_3 + \frac{1}{14} x_3 = -\varepsilon (d_6 x_1 x_2 + 2d_9 x_2 x_3). \end{cases} \quad (26)$$

It was shown in [Bruggeman & Verhulst, 2015] that for  $0 < u < \bar{u}$  we have  $d_6 < 0$ ,  $d_9 < 0$  and one of the short-periodic solutions is complex unstable. This is highly relevant for the characterization of the chaotic dynamics of the system as it was shown in [Hoveijn & Verhulst, 1990] that a Shilnikov–Devaney bifurcation [Devaney, 1976] will take place in the  $3 : 2 : 1$  resonance.

The analysis in [Hoveijn & Verhulst, 1990] is valid for the general time-independent Hamiltonian in  $3 : 2 : 1$  resonance. In the case of the special system (26) we give the following, simpler analysis. As discussed in [Bruggeman & Verhulst, 2015] we have directly from the intermediate normal form (26) the two normal modes:

- (1)  $x_1(t)$  nontrivial harmonic,  $x_2(t) = x_3(t) = 0$ ,  $t \geq 0$ ; stability  $HH$  (four real eigenvalues).
- (2)  $x_2(t) = r_0 \cos(\frac{2}{\sqrt{14}}t + \psi_0)$ ,  $x_1(t) = x_3(t) = 0$ ,  $t \geq 0$ ; stability  $C$  (four complex eigenvalues).

Also from [Bruggeman & Verhulst, 2015] we have four periodic solutions in general position, two stable and two unstable. In [Hoveijn & Verhulst, 1990] it is shown that there exist a family of homoclinic solutions of  $x_2$  when normalizing to  $H_3$ . Also, that when normalizing to  $H_4$  this family of homoclinic solutions breaks up into one transversal homoclinic producing the Shilnikov–Devaney result [Devaney, 1976] of a horseshoe map in the flow. The action simplex is shown in Fig. 16.

## 6.2. Numerical experiments for chaotic FPU-cells

Guided by the normal form of the  $3 : 2 : 1$  resonance we will demonstrate numerically a number of recurrence results for the original system of FPU-cells (7). We will choose particular but typical

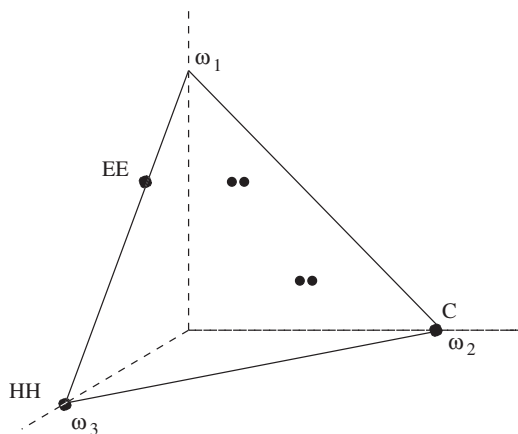


Fig. 16. The energy simplex for the  $3 : 2 : 1$  resonance;  $\omega_1 = 3/\sqrt{14}$ ,  $\omega_2 = 2/\sqrt{14}$ ,  $\omega_3 = 1/\sqrt{14}$ . Short-periodic solutions on the energy manifold are indicated by black dots. The  $x_2$  normal mode is complex unstable, the  $x_3$  normal mode is unstable with real eigenvalues. The short-periodic solution at  $x_2 = 0$  is stable. Of the four general position periodic solutions, two are stable, two unstable.

values for the masses, denoted in [Bruggeman & Verhulst, 2015] by “case 1”:

$$a_1 = 0.00510292, \quad a_2 = 0.117265,$$

$$a_3 = 0.0854008, \quad a_4 = 0.292231,$$

leading to the frequencies (25). With these mass ( $a_i$ ) values the symplectic transformation of the four-particles system in [Bruggeman & Verhulst, 2015] produces:

$$d_6 = -0.0306229, \quad d_9 = -0.0089438.$$

We will start with one cell; using the inverse symplectic transformation we have for the  $x_2$  normal mode at a fixed energy value:

$$\begin{aligned} x_2 : q_1(0) &= 0.00315777, \quad q_2(0) = -0.297518, \\ q_3(0) &= 0.126704, \quad q_4(0) = 0.127029. \end{aligned} \quad (27)$$

For the  $x_3$  normal mode we have:

$$\begin{aligned} x_3 : q_1(0) &= -0.0228266, \quad q_2(0) = 0.152804, \\ q_3(0) &= 0.235358, \quad q_4(0) = 0.121061. \end{aligned} \quad (28)$$

For the set-up of the numerical experiments we make the following observations. We will start with initial values in cell 1 and will be interested in recurrence and the energy transfer to cell 2. As the chain is Hamiltonian, the flow is recurrent, but we expect differences between the classical case of equal masses and the case of the  $3 : 2 : 1$  resonance where the flow is chaotic. We restrict ourselves to initial values in a neighborhood of the complex unstable normal mode.

The symplectic transformation  $L(u)$  from [Bruggeman & Verhulst, 2015] discussed in Sec. 6.1 gives us the relation between the normal modes of the system in quasi-harmonic coordinates  $(x, \dot{x})$  and the initial conditions in the variables  $(q, v)$  of system (7). This means that a given position vector  $(q_1, q_2, q_3, q_4) = \mathbf{q}$  is obtained from the  $\mathbf{x}$  normal modes by taking  $\mathbf{q} = L(u)\mathbf{x}$ . See for the initial data of our numerical experiments, Eq. (27). The  $3 : 2 : 1$  resonance will be detuned by the interaction between the cells. Keeping the interaction small by choosing  $\varepsilon c_1 = 0.1$ , the detuning does not disturb the qualitative picture of the flow. With the mass distribution of case 1 we have for the frequencies of the linearized system  $\omega_1 = 0.8018(0.8018)$ ,  $\omega_2 = 0.5354(0.5345)$ ,  $\omega_3 = 0.2677(0.2673)$  with between brackets the frequencies of isolated cells

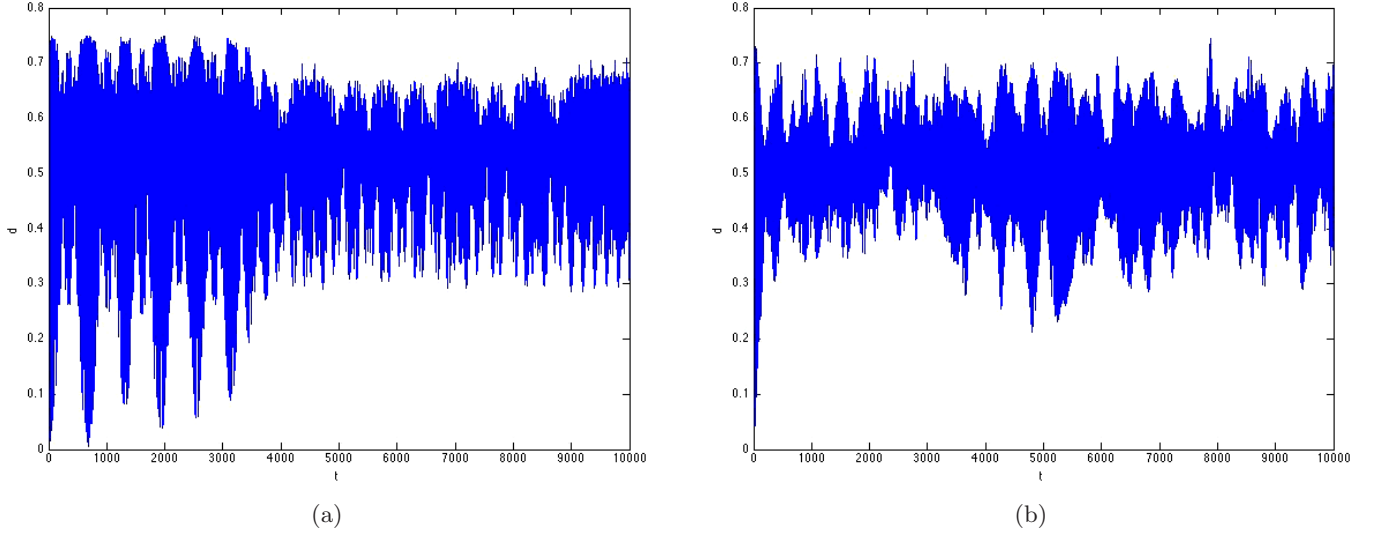


Fig. 17. Time series for the Euclidean distance in one and two cells based on system (3). Starting near the *complex unstable normal mode*, the initial conditions given by (27),  $\varepsilon = 1$ ,  $t \in [0, 10000]$ ; if  $d = 0.1$ ,  $L \sim 10^5$ . (a) One cell; first the normal mode is more or less followed for 3000 time steps, then the orbit wanders off; the accuracy (rel. error  $e^{-17}$ , abs. error  $e^{-20}$ ) does not permit continuation;  $H_2$  varies between 0.13 and 0.21. Recurrence will take a longer time. (b) The case of two cells; the  $1 : 2 : 3$  resonance is slightly detuned by choosing  $\varepsilon_{c1} = 0.1$ . With  $d = 0.1$ ,  $L = 10^{13}$ . The recurrence is delayed.

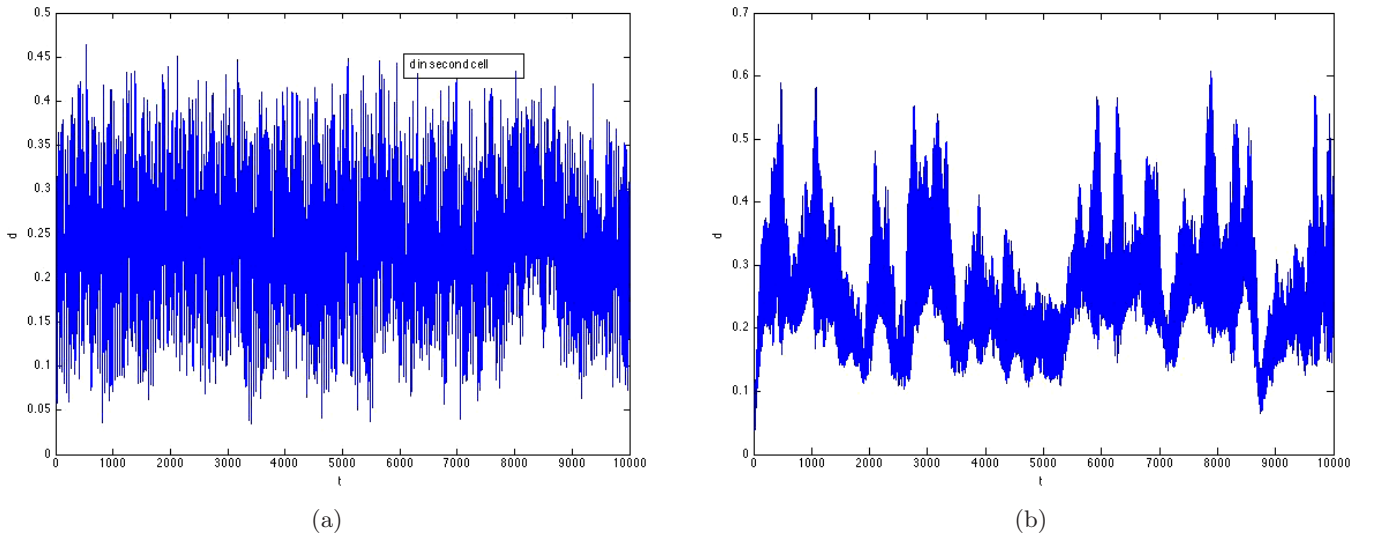


Fig. 18. Time series for the Euclidean distance in the second cell with initial conditions near the complex unstable normal mode and parameters as in Fig. 17. The energy transfer is quite strong but if  $\varepsilon_{c1} = 1$  (a) it is often exchanged with the first cell. (b) The case of slightly detuned and still chaotic  $1 : 2 : 3$  resonance  $\varepsilon_{c1} = 0.1$ .

( $c_1 = 0$ ). For reasons of comparison we also give the results when  $\varepsilon c_1 = 1$ ; in that case the  $1 : 2 : 3$  resonance of the first cell is heavily perturbed by linking it to the second cell. The strong perturbation of the resonance causes the energy obtained by the second cell to be more often returned to the first cell, see Fig. 18(a).

## 7. Conclusions

(1) It is easy to give a crude upper bound for the recurrence time on a bounded energy manifold near stable equilibrium of a Hamiltonian system. However, realistic bounds are strongly dependent on the resonances of the system and its near-integrability features. Normal forms play an essential part in identifying the near-integrability features showing strong differences between the cases of 2 and more dof. In a number of cases the recurrence time decreases with the energy but conjectures about recurrence times based on 2 dof experiments can be misleading for more dof.

(2) We have considered FPU-cells and FPU cell-chains (not to be confused with FPU chains). Three cases with different characteristics were considered.

- The FPU-cell with equal masses (the classical case) which is near-integrable. As expected this leads to relative short recurrence timescales for one cell. In the case of two cells quasi-trapping phenomena strongly delays recurrence.
- The Hamiltonian  $1 : 2 : 5$  resonance is an example of interesting behavior on different timescales. In the normal form to cubic terms of the Hamiltonian the 2 dof  $1 : 2$  resonance dominates, to first order this system is near-integrable. When normalizing to second order (the quartic terms) the third dof plays a part and this normal form is nonintegrable. In the case of a FPU-cell in  $1 : 2 : 5$  resonance this special Hamiltonian has similar features to the general case in [Haller & Wiggins, 1996].
- The FPU-cell in  $3 : 2 : 1$  resonance on the other hand has a chaotic first order normal form, resulting in much longer timescales.
- The fundamental concept of recurrence in Hamiltonian systems is not easy to use because of resonances and quasi-trapping. It would be interesting to explore the statistics of recurrence as discussed in [Zaslavsky, 2007, Chapters 6–7] for our three cases.

## Acknowledgments

Roelof Bruggeman provided a number of data and transformed systems to study FPU-cells, he also commented on the manuscript. Reinout Quispel kindly provided reference [Hairer *et al.*, 2006], an anonymous referee provided references [Christodoulidi *et al.*, 2010; Contopoulos & Polymilis, 1996], a second referee helpfully discussed estimate (11).

## References

- Bruggeman, R. & Verhulst, F. [2015] “The Inhomogeneous Fermi–Pasta–Ulam chain,” submitted, arXiv:1510.00560 [math.DS].
- Chechin, G. M. & Sakhnenko, V. P. [1998] “Interaction between normal modes in nonlinear dynamical systems with discrete symmetry. Exact results,” *Physica D* **117**, 43–76.
- Chechin, G. M., Novikova, N. V. & Abramenko, A. A. [2002] “Bushes of vibrational normal modes for Fermi–Pasta–Ulam chains,” *Physica D* **166**, 208–238.
- Christodoulidi, H., Efthymiopoulos, Ch. & Bountis, T. [2010] “Energy localization on  $q$ -tori, long-term stability, and the interpretation of Fermi–Pasta–Ulam recurrences,” *Phys. Rev. E* **81**, 6210.
- Contopoulos, G. & Polymilis, C. [1996] “Recurrence in the homoclinic tangle,” *Celest. Mech. Dyn. Astron.* **63**, 189–197.
- Devaney, R. L. [1976] “Homoclinic orbits in Hamiltonian systems,” *J. Diff. Eqs.* **21**, 431–438.
- Fermi, E., Pasta, J. & Ulam, S. [1955] “Los Alamos report LA-1940,” in *E. Fermi, Collected Papers*, Vol. 2, pp. 977–988.
- Ford, J. [1992] “The Fermi–Pasta–Ulam problem: Paradox turns discovery,” *Phys. Rep.* **213**, 271–310.
- Hairer, E., Lubich, C. & Wanner, G. [2006] *Geometric Numerical Integration*, 2nd edition (Springer).
- Haller, G. & Wiggins, S. [1996] “Geometry and chaos near resonant equilibria of 3-DOF Hamiltonian systems,” *Physica D* **90**, 319–365.
- Hoveijn, I. & Verhulst, F. [1990] “Chaos in the  $1 : 2 : 3$  Hamiltonian normal form,” *Physica D* **44**, 397–406.
- Poggi, P. & Ruffo, S. [1997] “Exact solutions in the FPU oscillator chain,” *Physica D* **103**, 251–272.
- Poincaré, H. [1892, 1893, 1899] *Les Méthodes Nouvelles de la Mécanique Céleste*, Vol. 3 (Gauthier-Villars, Paris).
- Rink, B. & Verhulst, F. [2000] “Near-integrability of periodic FPU-chains,” *Physica A* **285**, 467–482.
- Rink, B. [2001] “Symmetry and resonance in periodic FPU-chains,” *Commun. Math. Phys.* **218**, 665–685.
- Sanders, J. A., Verhulst, F. & Murdock, J. [2007] *Averaging Methods in Nonlinear Dynamical Systems*,

- Applied Mathematical Sciences, Vol. 59, 2nd edition (Springer).
- Van der Aa, E. & De Winkel, M. [1994] “Hamiltonian systems in  $1 : 2 : \omega$ -resonance,” *Int. J. Non-Linear Mech.* **29**, 261–270.
- Verhulst, F. [2015a] “Integrability and non-integrability of Hamiltonian normal forms,” *Acta Appl. Math.* **137**, 253–272.
- Verhulst, F. [2015b] “A chain of FPU-cells,” *Proc. 13th Int. Conf. Dynamical Systems — Theory and Applications*, eds. Awrejcewicz, J., Kazmierczak, M., Mrozowski, J. & Oleinik, P., Lodz, December 7–10, pp. 603–612. Extended version in *Applied Mathematical Modelling*, <http://dx.doi.org/10.1016/j.apm.2016.06.047>.
- Zaslavsky, G. M. [2007] *The Physics of Chaos in Hamiltonian Systems*, 2nd extended edition (Imperial College Press).